

We are IntechOpen, the world's leading publisher of Open Access books Built by scientists, for scientists

6,900

Open access books available

186,000

International authors and editors

200M

Downloads

Our authors are among the

154

Countries delivered to

TOP 1%

most cited scientists

12.2%

Contributors from top 500 universities



WEB OF SCIENCE™

Selection of our books indexed in the Book Citation Index
in Web of Science™ Core Collection (BKCI)

Interested in publishing with us?
Contact book.department@intechopen.com

Numbers displayed above are based on latest data collected.
For more information visit www.intechopen.com



Crystallization of Ge:Sb:Te Thin Films for Phase Change Memory Application

J. J. Gervacio Arciniega, E. Prokhorov, F. J. Espinoza Beltran and G. Trapaga
CINVESTAV, Unidad Queretaro, Juriquilla, Querétaro, Mexico

1. Introduction

Chalcogenide glasses are a chemical compound consisting of at least one chalcogen element, sulphur, selenium, or tellurium, in combination with other elements. These glasses obtained great attention after discovery between 1962 and 1969 by Kolomiets, Eaton, Ovshinsky and Pearson of the S-shape current-voltage characteristic in chalcogenide glasses and the switching phenomenon from high to low resistivity states (Popescu, 2005). In 1968 S. R. Ovshinsky demonstrated very short (about of 10^{-10} seconds) reversible electrical switching phenomena in $\text{Te}_{81}\text{Ge}_{15}\text{Sb}_2\text{S}_2$ thin films due to amorphous-crystalline phase transition (Ovshinsky, 1968). This work opened a new area of phase change technology, which now is one of the most important technologies for memory devices and applications in computers, CD, DVD, phase-change random access memories, etc.

The first electrical phase-change memory devices used various binary, ternary and quaternary Te-based films with compositions made up of Ge:Te, Si:As:Te, Ge:As:Si:Te, etc., systems (Stand, 2005). The early phase change materials used in optical storage comprised simple alloys based primarily on compositions in the vicinity of the tellurium-germanium eutectic. Antimony was primarily used, although other elements including selenium, arsenic and bismuth were all shown to have beneficial effects. Based on the results obtained from films with $\text{Ge}_{15}\text{Sb}_4\text{Te}_{81}$ composition (Ovshinsky, 1971) the first application of Ge:Sb:Te alloys was reported for phase change rewritable optical disks.

In the early 1990s, a second generation of high speed phase change materials based on Ge:Sb:Te alloys was reported by several optical memory research groups (Ohta et al 1989, Yamada et al, 1991, Gonzalez-Hernandez et al, 1992). These alloys have stoichiometric compositions along the GeTe-Sb₂Te₃ pseudobinary line of phase diagram such as $\text{Ge}_2\text{Sb}_2\text{Te}_5$, $\text{Ge}_1\text{Sb}_2\text{Te}_4$ and $\text{Ge}_1\text{Sb}_4\text{Te}_7$.

Ge:Sb:Te stoichiometric alloys have three phases: one amorphous and two crystal structures. The first crystalline phase is the rock salt NaCl-like and the second more stable phase is hexagonal. When the amorphous films are heated, the transition from amorphous to rock salt-like structure occurs at around 120-170°C; subsequent heating transforms this phase into a stable hexagonal structure at temperatures around 200-250°C. The exact transition temperature depends on the composition of the film. The hexagonal structure remains stable over a wide temperature range from 200-250°C to around the melting point (593-630 °C,

depending on composition) (Gonzalez-Hernandez et al, 1992). The principle of phase-change memory operation is based on a reversible phase-transformation from the amorphous (high resistance/low reflectivity state) to crystalline NaCl-type (low resistance/high reflectivity state) under short laser or electrical pulses. It is necessary to note that for phase-change memory applications only the amorphous-NaCl-type transition has been used, probably because the heating time produced by the laser or electrical pulse is too short to form the stable hexagonal structure (Yamada, 1991). This transformation is always accompanied by abrupt changes in reflection (about 20-30 %) and resistivity (about 3 orders of magnitude) in chalcogenide films. The reversible transformation from crystalline to the amorphous structurally disordered state can be obtained by increasing the local temperature of the Ge:Sb:Te layer above its melting point by short intense laser, or electrical pulses and the subsequent quenching with a cooling rate about 10^{10} deg/s (Yamada et al, 1991).

The phase transition between the amorphous and NaCl-type crystalline phase in stoichiometric materials is fast because atoms in the amorphous state do not need to travel long distances to take their position in the crystal lattice. On the other hand, non-stoichiometric compounds require long-range diffusion when they crystallize from an amorphous state (Yamada et al, 1991, Yamada 1996), which in general slows down the crystallization process. For example, 30 at. % of the deviation from $\text{Ge}_2\text{Sb}_2\text{Te}_5$ stoichiometric composition increased the crystallization time from 220 to 500 ns (Kyrsta et al., 2001).

For several years, Ge:Sb:Te alloys along the pseudobinary $\text{GeTe-Sb}_2\text{Te}_3$ line have been used as the main material for optical phase-change data storage devices and are currently being investigated for nonvolatile electronic storage purposes (which utilize the difference in the electrical resistance of the two phases) due to the high reflectivity and resistivity contrast between the amorphous and crystalline phases. Many investigations have been carried out on this type of phase-change materials with the purpose of improving their properties and to increase its storage capacity, stability, speed and versatility. These investigations have shown that the crystallization of the phase-change (or amorphous-NaCl-type transition) can be considered as a rate-limiting process to obtain a fast data transfer. That is why there are a considerable number of experimental and theoretical studies investigating the amorphous-to-crystalline NaCl-type phase transformation. In spite of the large number of publications, the activation energy for crystallization of Ge:Sb:Te materials reported in the literature shows a large discrepancy; the activation energy of crystallization for $\text{Ge}_2\text{Sb}_2\text{Te}_5$ reported in the literature varied between 0.8 and 2.9 eV, for example. Such dispersion in the kinetic parameters might depend on the differences in the deposition methods, type of substrate, dielectric cover layer, film thickness and/or parameters of deposition processes, which lead to differences in the crystallization temperature, activation energy, and the like. In addition, experimental data show relatively long incubation times for crystallization of Ge:Sb:Te films and a relatively large amount of crystallized material during this period of time (Morales-Sanchez et al 2010). Incubation time manifests itself as the time necessary to reach critical values of nucleus for the crystallization to occur (Senkader et al, 2004). The existence of a non-negligible amount of crystallite during the incubation time could also be responsible for the dispersion in the kinetic parameters reported in the literature.

Based on such antecedents, we aimed in this chapter at investigating the crystallization kinetics of thin films on a glass substrate obtained by the same deposition process (DC sputtering), with the same thickness (around 200 nm), and composition along the GeTe-

Sb_2Te_3 pseudobinary line ($\text{Ge}_2\text{Sb}_2\text{Te}_5$, $\text{Ge}_1\text{Sb}_2\text{Te}_4$ and $\text{Ge}_1\text{Sb}_4\text{Te}_7$) including GeTe and Sb_2Te_3 (which lie at the end of GeTe- Sb_2Te_3 pseudobinary line), taking into account the processes during the incubation time. It is necessary to note that GeTe and Sb_2Te_3 , as well as Ge:Sb:Te, can be used in phase-change data storage. Additionally, the crystallization kinetics of $\text{Ge}_4\text{Sb}_1\text{Te}_5$ films will be present in this chapter. The structure of this alloy is unclear. In contrast to other Ge:Sb:Te ternary compounds, it does not belong to the GeTe - Sb_2Te_3 homologous series, although it lies on (or very close to) the GeTe- Sb_2Te_3 pseudobinary line in the Ge:Sb:Te phase diagram between GeTe and $\text{Ge}_2\text{Sb}_2\text{Te}_5$. It is suggested (Coombs et al., 1995) that this alloy is a solid solution between GeTe and a compound with a composition close to $\text{Ge}_4\text{Sb}_1\text{Te}_5$. This material, in contrast to stoichiometric alloys, demonstrates only one amorphous-NaCl-type phase transition, but it has the largest optical (Kato et al., 1999) and electrical (Morales-Sanchez et al., 2005) contrast between the crystalline and amorphous states, compared with other Ge:Sb:Te ternary alloys.

Necessary to note that as-prepared and melt-quenched Ge:Sb:Te amorphous materials show different crystallization kinetics (Nobukuni et al., 1999, Park et al., 1999, Khulbe et al., 2000, Wei et al., 2003, Kalb et al., 2004, Raoux et al., 2008). It has been proposed in the literature that for melt-quenched amorphous materials may exist: embryos following the condensation and evaporation of embryos to form crystalline clusters (Khulbe et al., 2000), preexisting clusters (Park et al., 1999), crystal nuclei (Wei et al., 2003), sinks and voids after repeated overwriting (Nobukuni et al., 1999), locally ordered regions with structure similar to that of crystalline Sb (Naito et al., 2004) or a crystalline amorphous border (Raoux et al., 2008). In spite of different models, crystallization in the melt-quenched amorphous material can start from these nucleation centers, which decrease incubation time and increase crystallization speed. But in this chapter only crystallization of as-prepared materials will be discussed.

Studies of crystallization kinetics of phase change materials are mostly analyzed using the Johnson-Mehl-Avrami-Kolmogorov (JMAK) model for isothermal annealing (see for example: (Weidenhof et al., 2001, Ruitenbergh et al., 2002, Trappe et al., 2000, Morales-Sanchez et al., 2010)), which permitted to determine the activation energy for the crystallization process. This method will be used for investigation of the crystallization kinetics in the compositions mentioned above.

Figure 1 shows in-situ optical reflection (using a laser diode emitting at 650 nm) as a function of temperature with a heating rate of 5°C/min for all investigated films with composition indicated on the graph. An abrupt change in reflection is associated with the onset of phase crystallization. Stoichiometric $\text{Ge}_2\text{Sb}_2\text{Te}_5$, $\text{Ge}_1\text{Sb}_2\text{Te}_4$ and $\text{Ge}_1\text{Sb}_4\text{Te}_7$ materials demonstrate two changes: the first corresponds to amorphous-NaCl-type transition and the second to NaCl-type-hexagonal transformation. In contrast, GeTe, $\text{Ge}_4\text{Sb}_1\text{Te}_5$ and Sb_2Te_3 show only one amorphous-crystalline transition. The highest crystallization temperature (T_c) has been observed in GeTe, the lowest in Sb_2Te_3 . The crystallization kinetics of the GeTe- Sb_2Te_3 pseudobinary line will be analyzed according to this Figure from the highest to the lowest crystallization temperature.

2. Deposition of phase change films

An important aspect to develop thin films of phase change materials is the deposition method. It is well known from the literature that deposition technology strongly affects

the microstructure and as a result the optical, electrical and crystallization (especially the crystallization temperature) properties of phase-change materials. For example, the crystallization temperature of the films with the same composition but obtained by different deposition methods can differ for more than 20°C, and no suitable explanation has yet been proposed (Morales-Sanchez et al., 2005). That is why, to compare crystallization properties all studied films have to be obtained with the same deposition process (DC sputtering), with the same thickness (around 200 nm), and composition along the GeTe-Sb₂Te₃ pseudobinary line. This method has been chosen because sputtering can produce films with the desired stoichiometry. Compared, for example, with thermal evaporation, in sputtering the thickness and chemical composition of thin films are easier to control.

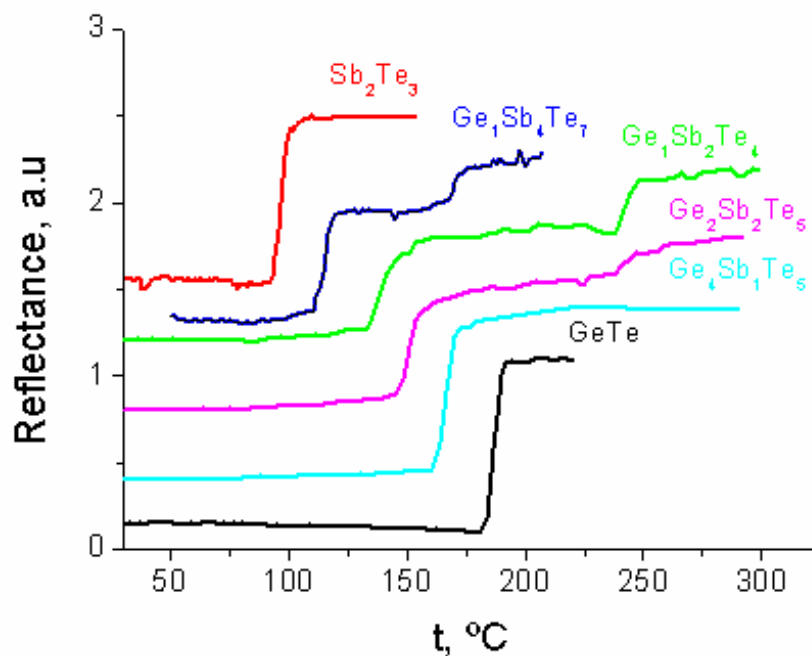


Fig. 1. Dependencies of optical reflection on temperature for films with compositions indicated on the graph.

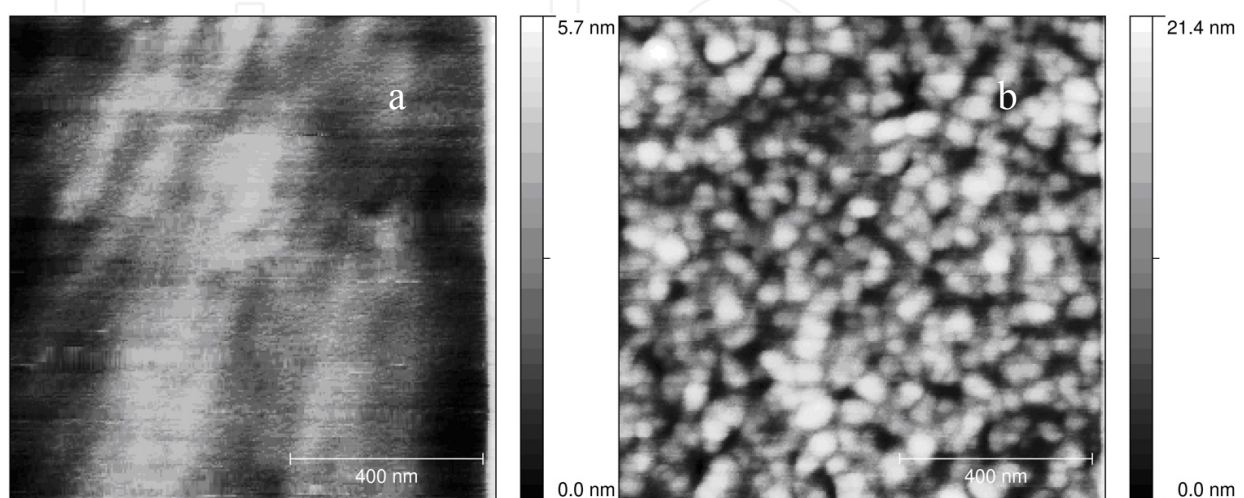


Fig. 2. Surface topography of as-prepared amorphous (a) and crystalline (b) Ge₂Sb₂Te₅ films.

The thin films have been prepared on glass and Si substrates by DC magnetron sputtering from one composite target. The deposition conditions were: 4.5×10^{-6} mbar base pressure, 2.0×10^{-5} mbar work pressure, 180 cm³/min Ar gas input flow, 0.49 W/cm² DC power density, and 10 min deposition time. Before films sputtering, the targets were cleaned for 10 minutes by sputtering to remove the oxide from the surface. According to XRD measurements all films were obtained in amorphous state. Energy dispersive spectroscopy has shown that deviations of films compositions from the targets were approximately 2%.

Figure 2a shows typical surface topography obtained from AFM measurements of as-prepared amorphous thin films. All amorphous films demonstrated very smooth surface with the surface roughness between 1 and 3 nm. In contrast, in the crystalline films (annealed to the temperature of 200°C) the topography image shows grains with average size between 20-120 nm (Fig. 2b). The dimensions of grains are dependent on the films composition.

3. Crystallization of GeTe

GeTe is a promising candidate for the application of in phase-change technology due to its higher crystallization temperature (onset of crystallization temperature at about 184°C) when compared to other alloys, since it offers a significant improvement in data-retention at high temperature (Perniola et al., 2010, Fantini et al., 2010). Amorphous films, in contrast to Ge:Sb:Te ternary alloys, crystallize in the rhombohedral phase. This phase can be viewed as a rock salt structure distorted along the [111]-direction (Caravati et al., 2010). Additionally, the central atom is displaced along the [111]-direction from the center of the rhombohedron. Upon crystallization, in a rhombohedral (distorted rock salt) structure appeared about 10% of vacancies occurring on Ge sites (Kolobov 2004). GeTe is a classical ferroelectric material that shows displacive type ferroelectric-paraelectric transition from a rhombohedral ferroelectric phase to a rock salt type structure with paraelectric properties. Two sublattices form this rock salt structure: Ge atoms compose one of the lattices and tellurium atoms the other (Rabe et al., 1987).

The NaCl type crystalline structure of GeTe is an unstable phase. This crystalline structure exists for temperatures above 300°C. The ferroelectric-paraelectric transition occurs in the interval of 327-427°C depending on various factors, such as exact composition, carrier density, etc. For example, changes in Te composition from 50 to 50.7 at. % shift the transition temperature from 427°C to 356°C (Okura, 1992).

Activation energy of amorphous to rhombohedral phase crystallization reported in the literature demonstrates large dispersion: 1.7 eV (Libera et al., 1993), 1.77 eV (Lu et al., 1995), 1.96 eV (Fantini et al., 2010), 2.5 eV (Fan et al., 2004), 3.9 eV (Matsushita et al., 1989). Such dispersion can be dependent on the differences in the deposition methods, type of substrate, method of results interpretation, etc. According to the literature and to our measurements (Fig. 1), GeTe has the highest crystallization temperature for materials on the GeTe-Sb₂Te₃ pseudobinary line and must demonstrate the highest activation energy of crystallization.

Figure 3 shows X-ray patterns of GeTe film measured at the temperature indicated on the graph. At temperatures below 180°C, the material shows only wide bands, which are characteristic of amorphous materials. At higher temperatures, a rhombohedral GeTe phase appears. At a temperature of 350°C two phases have been observed: rhombohedral and

NaCl-type, and at higher temperatures the material transforms into a NaCl-type phase. This phase exists only at temperatures above 400°C and in the process of cooling, again transforms into the stable rhombohedral phase.

Crystallization kinetics in GeTe, as in other materials, has been investigated using optical reflection during isothermal measurements. Reflection measurements were made with a 650 nm wavelength laser diode and a PIN diode as detector. In the reflectance measurements, the generally employed assumption has been used; the reflection signals are linearly related to the total transformed crystalline volume fractions x (Weidenhof et al., 2001):

$$x = [R(t) - R_a] / [R_c - R_a], \quad (1)$$

where $R(t)$, the experimental measurement value of reflectance, R_a and R_c are reflectance of amorphous and fully crystalline phases, respectively.

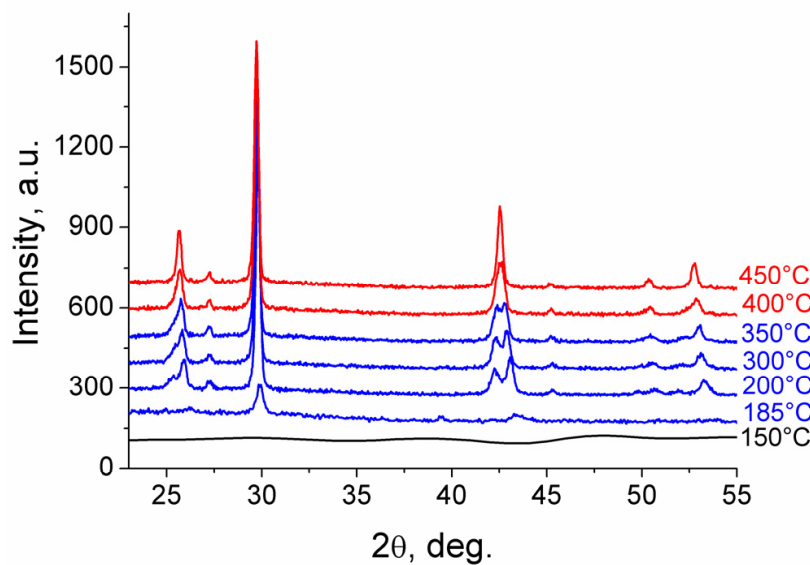


Fig. 3. XRD patterns of GeTe film measured at the temperature indicated on the graph. Blue patterns correspond to rhombohedral phase. Red patterns correspond to NaCl-type phase.

Figure 4 shows the evolution of the total crystalline volume fraction x , for GeTe samples, calculated from reflection measurements for films isothermally annealed at the temperatures indicated on the graph.

In this chapter, crystallization kinetics will be analyzed using the Johnson–Mehl–Avrami–Kolmogorov (JMAK) model for isothermal annealing. According to the classical JMAK model, the transformed volume fraction x can be determined by the following expression:

$$x(t) = 1 - \exp(-Kt^n), \quad (2)$$

where $K = \gamma \exp(-E/kT)$, γ is the frequency factor, E is the effective activation energy, t is the annealing time, and n the Avrami exponent, which provides information about the mechanisms of crystallization. The value of n can be evaluated from the slope of the $\ln[-\ln(1-x)]$ versus $\ln(t)$ plot, which in materials with random nucleation and isotropic growth should be linear. The JMAK model is based on several assumptions such as:

homogeneity of the system, random and uniform nucleation, and nucleation rate taking place at the very beginning of the transformation is time independent and applied for isotropic growth at a constant rate.

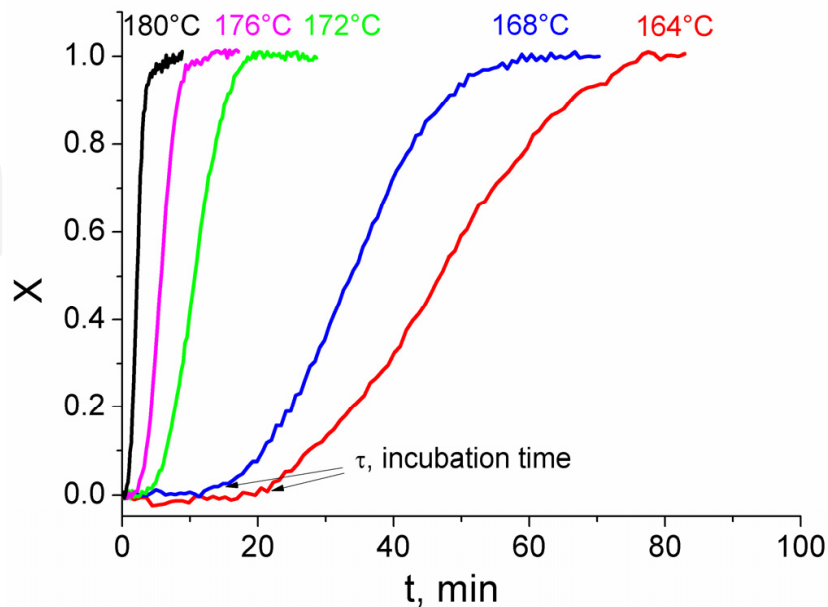


Fig. 4. Dependencies of the volume fraction x versus time obtained for GeTe samples from reflection measurements at the temperature indicated on the graph.

The value of activation energy for GeTe obtained using Equation (2) was very high: close to 12 eV. Such high value of activation energy has been obtained because GeTe, as other Ge:Sb:Te materials, shows long incubation times τ for crystallization, namely, the annealing time required to reach a critical nuclei size or to observe an abrupt increase in the crystalline volume fraction. In this case, the nucleation rate cannot be considered to be time independent for the entire crystallization process as is considered in classical JMAK models (Senkader et al., 2004).

In the case of GeTe, the volume fraction of crystalline phase approximately equals zero during all the incubation time (see Fig. 4). In such cases than the volume fraction of crystalline phase does not demonstrate a substantial increase during the incubation time it is possible to define the beginning of the transformation after the incubation time (Weidenhof et al., 2001). The JMAK equation can now be expressed as:

$$x(t) = 1 - \exp[-K(t - \tau)^n], \quad (3)$$

where τ is the incubation time. According to Equation (3) the plot $\ln[-\ln(1-x)]$ versus $\ln(t-\tau)$ must be a straight line with slope n . Figure 5 shows such modification of an Avrami plot for GeTe. The insert shows the rate constant as a function of the reciprocal temperature.

The calculated activation energy for GeTe as determined from the modification of the Avrami Equation (3) using the Arrhenius type relation for K was 3.98 ± 0.12 eV. The value of the Avrami exponent was about 1.6, which corresponds to diffusion controlled growth from small dimension grains with decreasing nucleation rate (Christian, 1975).

In addition, X-ray measurements have shown that during isothermal annealing from amorphous phase only one rhombohedral phase appeared. As time increases, the volume fraction of amorphous phase decreases (Figure 6); in the same time, the volume fraction of crystalline phase increases. No shift in the position of diffraction peaks was observed. This observation will be important in the analysis of crystallization processes of $\text{Ge}_2\text{Sb}_2\text{Te}_5$ and $\text{Ge}_1\text{Sb}_2\text{Te}_4$ materials.

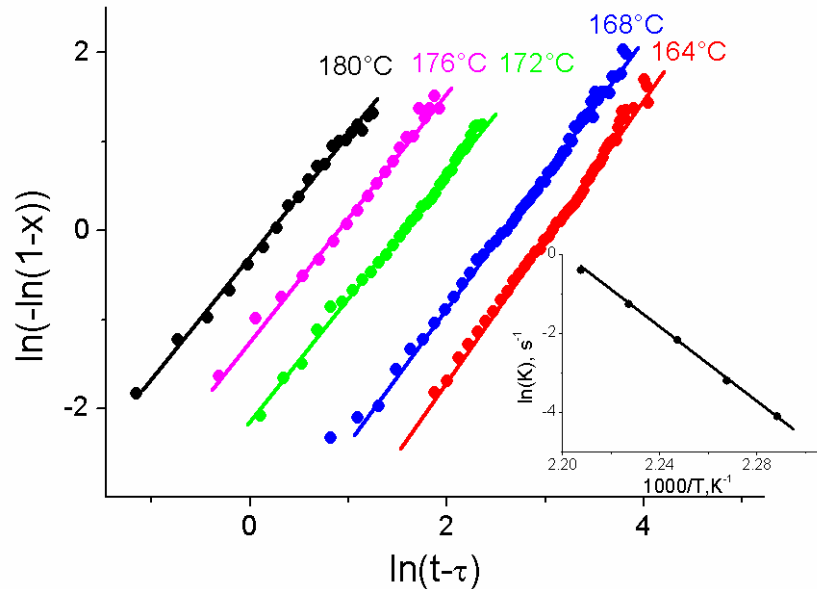


Fig. 5. Avrami plot of $\ln[-\ln(1-x)]$ vs $\ln(t-\tau)$ for GeTe. Points – experiment, lines – result of fitting using JMAK equation (3). The insert shows the rate constant K as function of the reciprocal temperature.

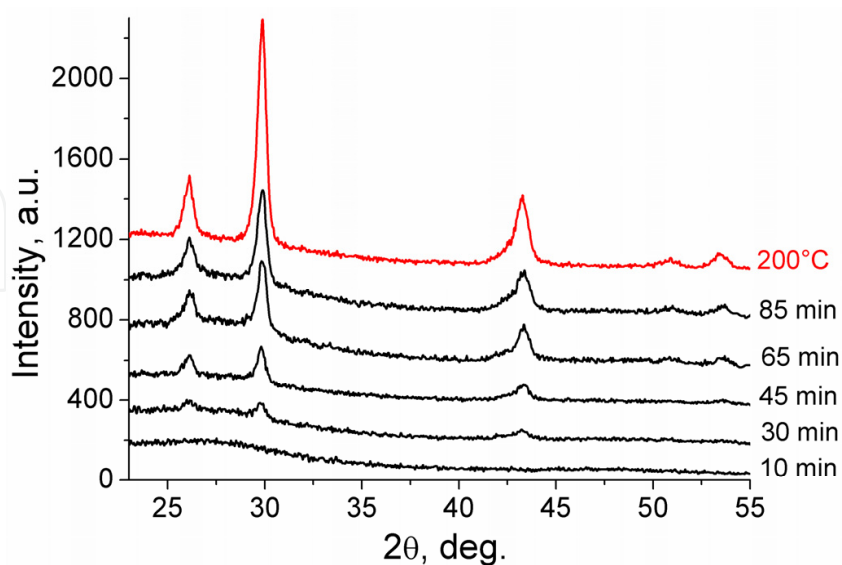


Fig. 6. X-ray diffraction spectra for a GeTe film obtained in the process of isothermal annealing at a temperature of 164°C during the time indicated on the plot. The upper pattern corresponds to film annealing at 200°C .

4. Crystallization of $\text{Ge}_4\text{Sb}_1\text{Te}_5$

As mentioned above, the structure of $\text{Ge}_4\text{Sb}_1\text{Te}_5$ is not known. It lies on or is close to the $\text{GeTe-Sb}_2\text{Te}_3$ pseudobinary line in the Ge:Sb:Te phase diagram between GeTe and $\text{Ge}_2\text{Sb}_2\text{Te}_5$. Because of such position, the onset of crystallization temperature is about 160°C , less than in GeTe but higher than in another Ge:Sb:Te ternary alloys. This alloy crystallizes in NaCl-type structure (Gonzalez-Hernandez et al., 1992, Wamwangi et al., 2002, Ruiz Santos et al., 2010). For $\text{Ge}_4\text{Sb}_1\text{Te}_5$ films the reported values of the activation energy varied in a wide range: 1.13 eV (Kato et al., 1999), 3.09 eV (Morales-Sanchez et al., 2005), 3.48 eV (Wamwangi et al., 2002).

In addition, similarly to GeTe, bulk material and thin $\text{Ge}_4\text{Sb}_1\text{Te}_5$ films demonstrate at a temperature of approximately 327°C ferroelectric-paraelectric transition (Bahgat et al., 2004, Ruiz Santos et al., 2010). But in contrast to GeTe, in which ferroelectric-paraelectric transition relates to a transformation from a rhombohedral phase to a rock salt type structure, in $\text{Ge}_4\text{Sb}_1\text{Te}_5$ the ferroelectric-paraelectric transition relates to a transformation between two different rock salt type structures.

Figure 7 shows DSC measurements on a crystalline $\text{Ge}_4\text{Sb}_1\text{Te}_5$ bulk alloy and on the amorphous material obtained by removing the as-deposited films from the glass substrates. In the bulk alloys, a nonsymmetrical endothermic peak at a temperature of 329°C has been observed. In contrast, DSC measurements on amorphous material showed an exothermic peak at 176°C , which is associated with the crystallization of the sample and a broad endothermic peak, with a maximum at approximately 327°C , and that corresponds to the same temperature as in the bulk alloy. The observed endothermic peak can be associated with the ferroelectric-paraelectric transition.

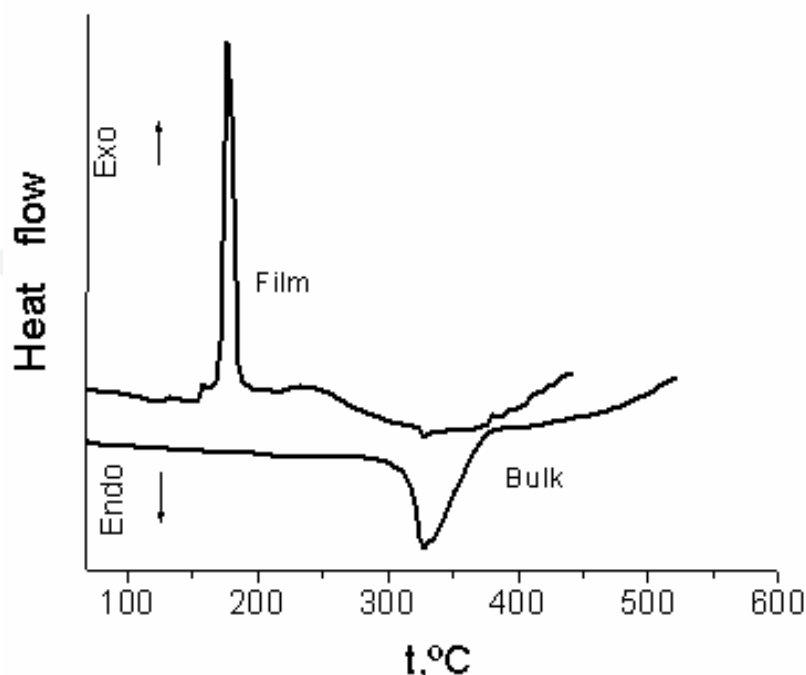


Fig. 7. DSC measurements on a bulk crystalline alloy and on the amorphous material, obtained by removing the as-deposited films from the glass substrates.

Additional confirmation of ferroelectric-paraelectric transition in $\text{Ge}_4\text{Sb}_1\text{Te}_5$ films has been obtained by temperature capacitance measurements (Ruiz Santos et al., 2010). In this work, it has been shown that the reciprocal capacitances (which are proportional to the reciprocal dielectric constant) as a function of temperature show a typical Curie-Weiss behavior for temperatures above 327°C .

Specific data of crystallization process and ferroelectric-paraelectric transition in $\text{Ge}_4\text{Sb}_1\text{Te}_5$ films can be obtained by in situ XRD measurements at different temperatures. Figure 8 shows that below the crystallization temperature the film is in an amorphous state (pattern at 140°C). As the temperature is increased, the material crystallizes in the NaCl type structure. As the temperature continues increasing, the position of all $\text{Ge}_4\text{Sb}_1\text{Te}_5$ peaks shift to lower 2θ values, reaching saturation at a temperature of approximately 327°C at positions close to the NaCl type of GeTe structure (ICSD card #602124), which demonstrate paraelectric properties. The position of the NaCl type of GeTe is marked on the graph with the horizontal line. This shift can be clearly seen on the insert of Figure 8, which shows the temperature dependence of the (200) diffraction peak in $\text{Ge}_4\text{Sb}_1\text{Te}_5$. The horizontal line on the insert indicates the position of the (200) peak in crystalline GeTe.

Figure 9 shows the evolution of the total crystalline volume fraction x , for $\text{Ge}_4\text{Sb}_1\text{Te}_5$ samples, calculated from reflection measurements for films isothermally annealed at temperatures indicated on the graph. As in the case of GeTe, the volume fraction of crystalline phase of $\text{Ge}_4\text{Sb}_1\text{Te}_5$ is approximately equal to zero during all the incubation time. The same as for GeTe, kinetics parameters for $\text{Ge}_4\text{Sb}_1\text{Te}_5$ can be calculated using Eq. (3).

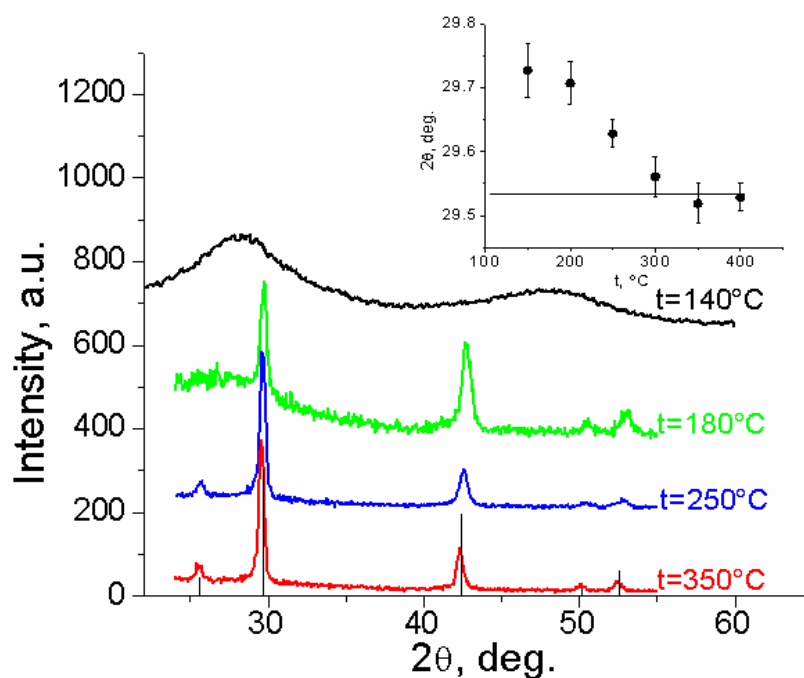


Fig. 8. XRD patterns of $\text{Ge}_4\text{Sb}_1\text{Te}_5$ film measured at the temperature indicated on the graph. The insert shows temperature dependence of (200) diffraction line in $\text{Ge}_4\text{Sb}_1\text{Te}_5$.

Figure 10 shows the modification of an Avrami plot for $\text{Ge}_4\text{Sb}_1\text{Te}_5$. The insert shows the rate constant as a function of the reciprocal temperature. The effective activation energy, determined from the Avrami plot for different temperatures using the Arrhenius type

relation for K , was 3.46 ± 0.22 eV (insert in Fig. 10). This value is in good agreement with other values reported in the literature ($3.48 \text{ eV} \pm 0.12 \text{ eV}$) obtained using the Kissinger analysis (Wamwangi et al., 2002). The Avrami exponent for $\text{Ge}_4\text{Sb}_1\text{Te}_5$ was close to 1.8, which corresponds to a diffusion controlled growth from small dimension grains with decreasing nucleation rate, an exponent similar to that of GeTe (Christian 1975).

Additional X-ray measurements have shown that during isothermal annealing from amorphous phase only one NaCl-type phase appeared.

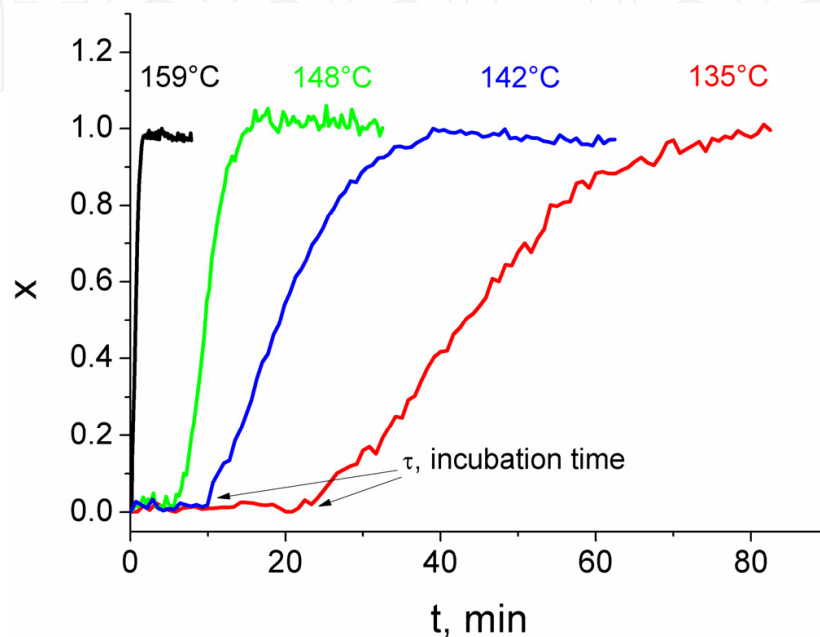


Fig. 9. Dependencies of the volume fraction x versus time obtained for $\text{Ge}_4\text{Sb}_1\text{Te}_5$ samples from reflection measurements at the temperature indicated on the graph.

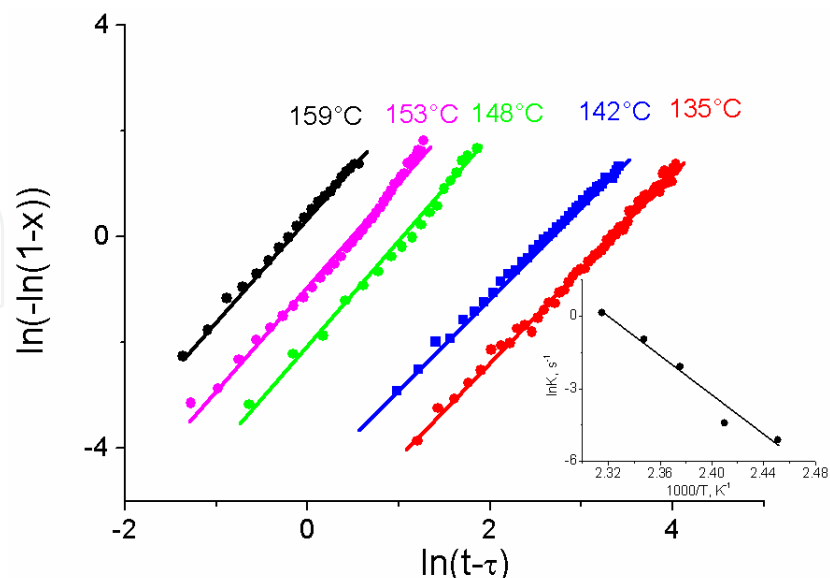


Fig. 10. Avrami plot of $\ln[-\ln(1-x)]$ vs $\ln(t-\tau)$ for $\text{Ge}_4\text{Sb}_1\text{Te}_5$ films. Points - experiment, lines - results of fitting using JMAK equation (3). The insert shows the rate constant K as function of the reciprocal temperature.

5. Crystallization of $\text{Ge}_2\text{Sb}_2\text{Te}_5$

$\text{Ge}_2\text{Sb}_2\text{Te}_5$ thin films are the most commonly employed materials for phase-change memory technology application due to its high crystallization speed and relatively high crystallization temperature (but less than in GeTe and $\text{Ge}_4\text{Sb}_1\text{Te}_5$), which lead to high thermal stability. Because of this, many extensive experimental and theoretical studies have been conducted to understand the structure and crystallization phenomena in this material (see for example (Yamada et al., 1991, Weidenhof et al., 2001, Matsunaga et al., 2004, Matsunaga et al., 2006, Paesler et al., 2007, Im et al., 2008, Claudio et al 2006)).

As mentioned above, $\text{Ge}_2\text{Sb}_2\text{Te}_5$ material demonstrates two phase changes: first at a temperature close to 145°C there is an amorphous-NaCl-type transition and second (at about 240°C) a NaCl-type-hexagonal transformation.

Under heating, the amorphous $\text{Ge}_2\text{Sb}_2\text{Te}_5$ films crystallize at around $130\text{-}170^\circ\text{C}$, depending on the preparation method and heating rate, into a phase with a NaCl-type structure ($Fm\bar{3}m$). In this structure, the 4(a) site is fully occupied by Te atoms, whereas the 4(b) site is randomly occupied by Ge and Sb atoms and vacancies. The composition of Ge:Sb:Te ternary system, which lie on the GeTe-Sb₂Te₃ pseudobinary line, can be described as $(\text{GeTe})_x + (\text{Sb}_2\text{Te}_3)_{1-x}$ ($0 < x < 1$). In such case the site occupancy of the vacancy varies continuously according to $(1-x)/(3-2x)$ (Matsunaga et al., 2004, Matsunaga et al., 2006). But Ge and Sb atoms deviate from the ideal rock-salt positions in $\text{Ge}_2\text{Sb}_2\text{Te}_5$ not in a random way but in a strongly correlated manner with respect to the neighboring Te atoms (Kolobov et al., 2004, Kolobov et al., 2006). The off-center location of Ge atoms means that there is a net dipole moment and suggests that a NaCl-type phase of the $\text{Ge}_2\text{Sb}_2\text{Te}_5$ is a ferroelectric material (Tominaga et al., 2004). The ferroelectric properties in $\text{Ge}_2\text{Sb}_2\text{Te}_5$ NaCl-type phase have been observed using capacitance-temperature measurements. The temperature dependence of the capacitance shows an abrupt change with a maximum at the temperature that corresponds to the end from a NaCl-type to a hexagonal transition. In addition, the reciprocal capacitance for temperatures above this transition shows the Curie-Weiss dependence, which is typical of ferroelectric materials (Gervacio Arciniega et al., 2010).

In spite of the large number of publications about crystallization phenomena in $\text{Ge}_2\text{Sb}_2\text{Te}_5$, the activation energy of crystallization reported in the literature shows a large discrepancy in the range between 0.8 and 2.9 eV and between 1.2 and 4.4 for the Avrami exponent (Morales-Sanchez et al., 2010, Liu et al., 2009). Such parameter dispersion can be related not only to the difference in the preparation methods but to the specific crystallization process.

Experimental data in $\text{Ge}_2\text{Sb}_2\text{Te}_5$ films, as in all materials along the pseudobinary GeTe-Sb₂Te₃ line, show relatively long incubation times during isothermal crystallization (Weidenhof et al., 2001, Laine et al., 2004, Zhang et al., 2008, Morales-Sanchez et al., 2010). But in GeTe and $\text{Ge}_4\text{Sb}_1\text{Te}_5$ the amount of crystallized material is close to zero during the incubation. In contrast, in $\text{Ge}_2\text{Sb}_2\text{Te}_5$ films large amount of crystallized material has been observed during this period of time (ranging from 50% in Ref. (Zhang et al., 2008), 10% in Ref. (Sian et al., 2008), 9% in Ref. (Laine et al., 2004) and 8% in Ref. (Weidenhof et al., 2001)). It is necessary to note that the amount of crystalline phase material during incubation time depends on the annealing temperature. The existence of a non-negligible amount of

crystallite during the incubation time, as will be shown below, is the most important factor responsible for the dispersion in the kinetic parameters reported in the literature.

Figure 11 shows the evolution of the total crystalline volume fraction x , for $\text{Ge}_2\text{Sb}_2\text{Te}_5$ samples, calculated from reflection measurements for films isothermally annealed at the temperatures indicated on the graph. In contrast to GeTe and $\text{Ge}_4\text{Sb}_1\text{Te}_5$, the volume fraction of crystalline phase of $\text{Ge}_2\text{Sb}_2\text{Te}_5$ does not equal zero during incubation time.

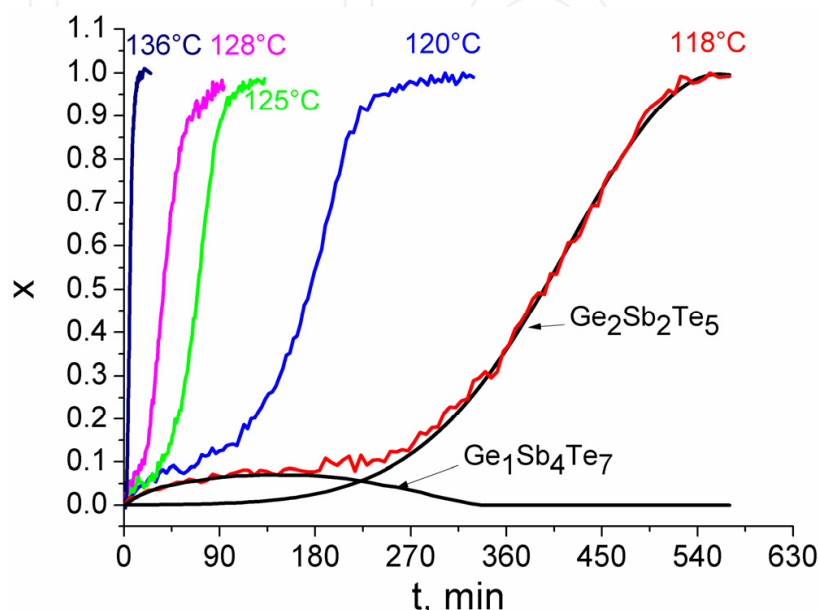


Fig. 11. Dependencies of the volume fraction x versus time obtained for $\text{Ge}_2\text{Sb}_2\text{Te}_5$ samples from reflection measurements at the temperature indicated on the graph. Black curves results from fittings using equation (7).

A typical JMAK plot for $\text{Ge}_2\text{Sb}_2\text{Te}_5$ films is shown in Figure 12. If we evaluate the slope only on a linear behavior, which is observed after incubation time τ , using a classical equation (2), the effective activation energy and the Avrami exponent will be equal to 5.61 eV and 3.3, respectively. The evaluation using a modification of a JMAK equation (3), which takes into account the incubation time, renders values for effective activation energy and an Avrami exponent equal to 2.07 eV and 1.5, respectively. This value of activation energy correlates well with what is reported in the literature (2.0 eV) and is obtained from the same interpretation of the reflection measurements (Weidenhof et al., 2001). Thus what comes into question is the pertinence of using these two approximations.

As has been mentioned above, the JMAK model is based on the following assumptions: the system is homogeneous, nucleation is random and uniform, the nucleation rate is time independent and takes place at the very beginning of the transformation, the isotropic growth maintains a constant rate, etc. (Henderson, 1979). However, nucleation in $\text{Ge}_2\text{Sb}_2\text{Te}_5$ films is not random nor uniform (Senkader et al., 2004) and due to partial crystallization during incubation time the nucleation rate cannot be considered to be time independent for the entire crystallization process as is considered in the classical model (equation 2). To overcome this limitation it has been proposed to avoid using a modification of the JMAK model (equation 3): after incubation time the rate constant can be considered as independent in time (Weidenhof et al., 2001). But in the case of $\text{Ge}_2\text{Sb}_2\text{Te}_5$ a large amount of crystallized

material has been observed during incubation time. Moreover, experimental investigation has shown that nuclei, which appeared in $\text{Ge}_2\text{Sb}_2\text{Te}_5$ films during incubation time, have a composition corresponding to $\text{Ge}_1\text{Sb}_4\text{Te}_7$ which differs from the nominal value for the amorphous matrix (Laine et al., 2004, Claudio et al., 2006). Figure 13 shows X-ray diffraction patterns for $\text{Ge}_2\text{Sb}_2\text{Te}_5$ film isothermal annealing at the temperature 118°C and times indicated on the graph. The patterns of samples annealed during 50, 100, and 200 minutes show weak peaks, with positions corresponding to $\text{Ge}_1\text{Sb}_4\text{Te}_7$ NaCl-type phase. After annealing for more than 200 min, the positions of the peaks begin to change to those

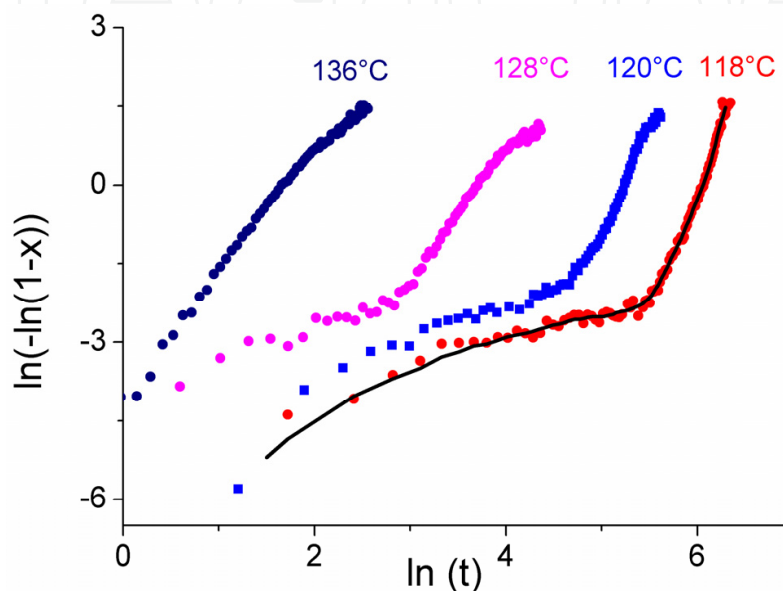


Fig. 12. Avrami plot of $\ln[-\ln(1-x)]$ vs $\ln(t)$ for $\text{Ge}_2\text{Sb}_2\text{Te}_5$ films. Points - experiment, black line - results of fitting using equation (7).

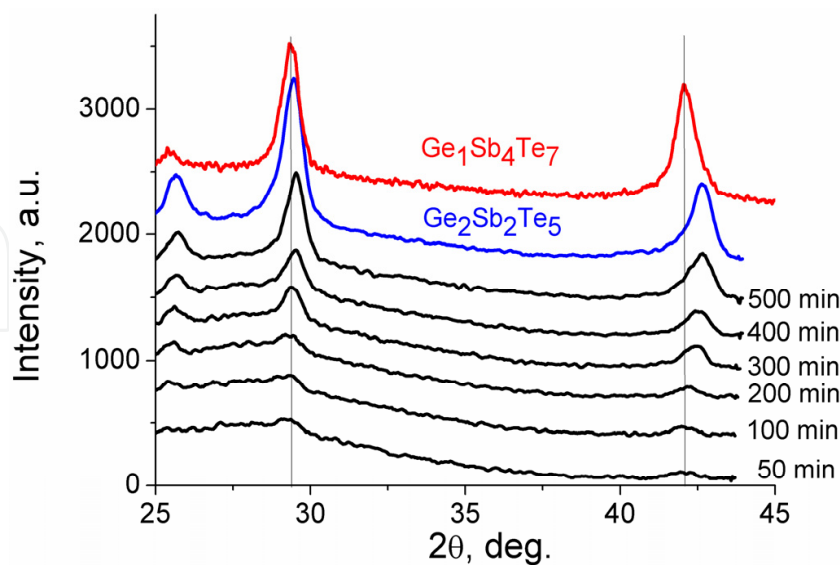


Fig. 13. X-ray diffraction spectra for a $\text{Ge}_2\text{Sb}_2\text{Te}_5$ film obtained in the process of isothermal annealing at a temperature of 118°C during the time indicated in the plot. Upper patterns correspond to $\text{Ge}_1\text{Sb}_4\text{Te}_7$ (red curve) and $\text{Ge}_2\text{Sb}_2\text{Te}_5$ (blue curve) taken at 180°C . The positions of the $\text{Ge}_1\text{Sb}_4\text{Te}_7$ peaks are indicated with the vertical lines.

corresponding to the NaCl-type phase of $\text{Ge}_2\text{Sb}_2\text{Te}_5$ composition. In this figure the blue pattern corresponds to material annealed at 180°C ; the upper pattern corresponds to $\text{Ge}_1\text{Sb}_4\text{Te}_7$ film annealed at 180°C . Thus, in $\text{Ge}_2\text{Sb}_2\text{Te}_5$ films the formation of a stable rock salt type crystalline phase is preceded by the formation of a metastable $\text{Ge}_1\text{Sb}_4\text{Te}_7$ phase.

On the basis of these results, the crystallization of $\text{Ge}_2\text{Sb}_2\text{Te}_5$ material during isothermal annealing can be considered as a process which takes place in two stages: in the first stage nuclei of a metastable $\text{Ge}_1\text{Sb}_4\text{Te}_7$ phase appear; in the second stage, the nuclei transform into the equilibrium NaCl-type stoichiometric $\text{Ge}_2\text{Sb}_2\text{Te}_5$ structures.

In materials in which phase transformation starts with the formation of metastable phases the isothermal crystallization process cannot be simply described by JMAK theory and the plots of $\ln(-\ln(1-x))$ versus $\ln(t)$ are not linear, which implies that the Avrami exponent n does not remain constant during the crystallization process.

In ref. (Claudio et al., 2006) an analytical model that can describe the isothermal crystallization process of materials is proposed. In this process, the stable crystalline phase is preceded by the formation of a metastable phase. The model assumes that the volume fraction of metastable phase f_m grows up to a maximum value f_{max} and then stops growing when the stable phase that has nucleated into it overpasses the metastable grain boundaries. The kinetics of the metastable fraction can be represented by a JMAK-type equation subtracting the fraction of stable phase f_{sm} which grows inside the metastable phase:

$$f_m(t) = f_{max}(1 - \exp(-K_m t^{n_m})) - f_{sm}(t), \quad (4)$$

where K_m is the crystallization rate constant and n_m the Avrami exponent.

The kinetic behavior of the stable phase into a metastable phase can be represented by the modification of classical JMAK formula, which takes into account the incubation time t_{sm} of the stable phase into the metastable phase:

$$\begin{aligned} f_{sm}(t) &= f_{max}(1 - \exp(-K_{sm}(t - t_{sm})^{n_{sm}})) \quad \text{for } t \geq t_{sm} \\ \text{and } f_{sm}(t) &= 0 \quad \text{for } t < t_{sm} \end{aligned} \quad (5)$$

where K_{sm} and n_{sm} are the crystallization rate constant and the Avrami exponent, respectively, which represent the kinetic parameters of the transformation from stable phase into metastable phase.

Furthermore, it is possible to propose that the stable phase can grow into the amorphous phase. The stable phase transformation kinetics in amorphous phase can be described by JMAK-type equation with its specific parameters:

$$\begin{aligned} f_{sa}(t) &= (1 - f_{max})(1 - \exp(-K_{sa}(t - t_{sa})^{n_{sa}})) \quad \text{for } t \geq t_{sa} \\ \text{and } f_{sa}(t) &= 0 \quad \text{for } t < t_{sa} \end{aligned} \quad (6)$$

where f_{sa} is the fraction of the stable phase in amorphous phase (from 0 to $1-f_{max}$), K_{sa} and n_{sa} are the JMAK parameters and t_{sa} is the incubation time of stable phase in amorphous phase.

The total fraction of transformed material is given by the equation:

$$f_{total}(t) = f_m(t) + f_{sm}(t) + f_{sa}(t) \quad (7)$$

This model allows fitting the experimental transformation data obtained in $\text{Ge}_2\text{Sb}_2\text{Te}_5$ films using a genetic algorithm. The continuous lines on Fig. 11 show the evolution on time of the volume fractions of metastable $\text{Ge}_1\text{Sb}_4\text{Te}_7$ and stable $\text{Ge}_2\text{Sb}_2\text{Te}_5$ phase obtained from fitting using Equation (7). Results of simulations have shown that the volume fraction of metastable $\text{Ge}_1\text{Sb}_4\text{Te}_7$ phase grows up to a maximum value and then decreases and disappears. After some incubation time, the $\text{Ge}_2\text{Sb}_2\text{Te}_5$ phase began to grow and all material is transformed into a stable crystalline phase.

In addition, the model is capable of predicting the three slopes clearly shown in the JMAK plot (Fig. 12) corresponding to three distinguishable stages in the crystallization process observed at dependencies obtained at low annealing temperature: the first one related to the metastable transformation, the second one (low value) with the step between metastable and stable transformation, and the last one with the stable phase nucleation and growth. It is quite evident from these simulated results that the first slope of the JMAK plot can be related to the kinetic behavior of the metastable phase.

The results of the investigation have shown that during the isothermal process of amorphous to crystalline phase transformation in $\text{Ge}_2\text{Sb}_2\text{Te}_5$ film a metastable phase with composition $\text{Ge}_1\text{Sb}_4\text{Te}_7$ and a stable NaCl-type $\text{Ge}_2\text{Sb}_2\text{Te}_5$ phase coexist within a certain time range. The appearance of nuclei of the $\text{Ge}_1\text{Sb}_4\text{Te}_7$ composition could be related to the local fluctuation in the film composition and to the fact that the crystallization temperature of $\text{Ge}_1\text{Sb}_4\text{Te}_7$ is lower than in $\text{Ge}_2\text{Sb}_2\text{Te}_5$ material.

6. Crystallization of $\text{Ge}_1\text{Sb}_2\text{Te}_4$

$\text{Ge}_1\text{Sb}_2\text{Te}_4$, as with $\text{Ge}_2\text{Sb}_2\text{Te}_5$ film, during annealing crystallize at a temperature of approximately 133°C (lower than the crystallization temperature of $\text{Ge}_2\text{Sb}_2\text{Te}_5$) into a NaCl-type structure ($Fm\bar{3}m$) (Matsunaga et al., 2004) and at a higher temperature (about 235°C) into a hexagonal phase. Because of the lower crystallization temperature, if compared with $\text{Ge}_2\text{Sb}_2\text{Te}_5$, this material may possess a low programming current in random access memory.

Crystallization kinetics, the same as in $\text{Ge}_2\text{Sb}_2\text{Te}_5$ material, is sufficiently complicated. Figure 14 shows the dependence of the total crystalline volume fraction x versus time for $\text{Ge}_1\text{Sb}_2\text{Te}_4$ samples calculated from reflection measurements for films isothermally annealed at the temperatures indicated on the graph and Figure 15 shows a typical JMAK plot. If we evaluate the slope only on a linear behavior, which is observed after incubation time τ , using classical equation (2), the effective activation energy will be equal to 5.45 eV. The evaluation using modification of JMAK equation (3), which takes into account incubation time, renders values of effective activation energy equal to 1.77 eV. But in $\text{Ge}_1\text{Sb}_2\text{Te}_4$, the same as in $\text{Ge}_2\text{Sb}_2\text{Te}_5$ films, a large amount of crystallized material has been observed during the incubation time. Moreover, XRD measurements (Figure 16) have shown that nuclei, which appeared in $\text{Ge}_1\text{Sb}_2\text{Te}_4$ films during the incubation period, have a composition corresponding to the $\text{Ge}_1\text{Sb}_4\text{Te}_7$ structure. The upper XRD pattern in this Figure corresponds to a fully crystallized film with the $\text{Ge}_1\text{Sb}_4\text{Te}_7$ composition; the peak positions of this phase are marked with the vertical lines. The pattern mark as $\text{Ge}_1\text{Sb}_2\text{Te}_4$ shows diffraction lines of $\text{Ge}_1\text{Sb}_2\text{Te}_4$ film annealing to 180°C .

The results obtained have shown that in $\text{Ge}_1\text{Sb}_2\text{Te}_4$, the same as in $\text{Ge}_2\text{Sb}_2\text{Te}_5$ film, during the isothermal process of amorphous to crystalline phase transformation, a metastable phase appeared with composition of $\text{Ge}_1\text{Sb}_4\text{Te}_7$. Thus, for the interpretation of the crystallization process in $\text{Ge}_1\text{Sb}_2\text{Te}_4$ an analytical model can be used in which the formation during crystallization of metastable phase is taken into account (Equation 7).

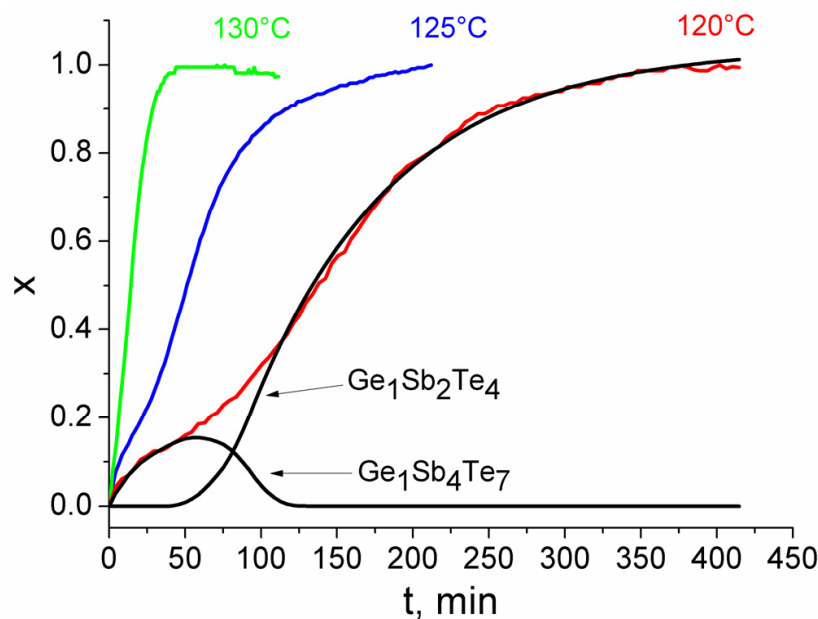


Fig. 14. Dependencies of the volume fraction x versus time obtained for $\text{Ge}_1\text{Sb}_2\text{Te}_4$ samples from reflection measurements at the temperature indicated on the graph. Black curves – results from fittings using equation (7).

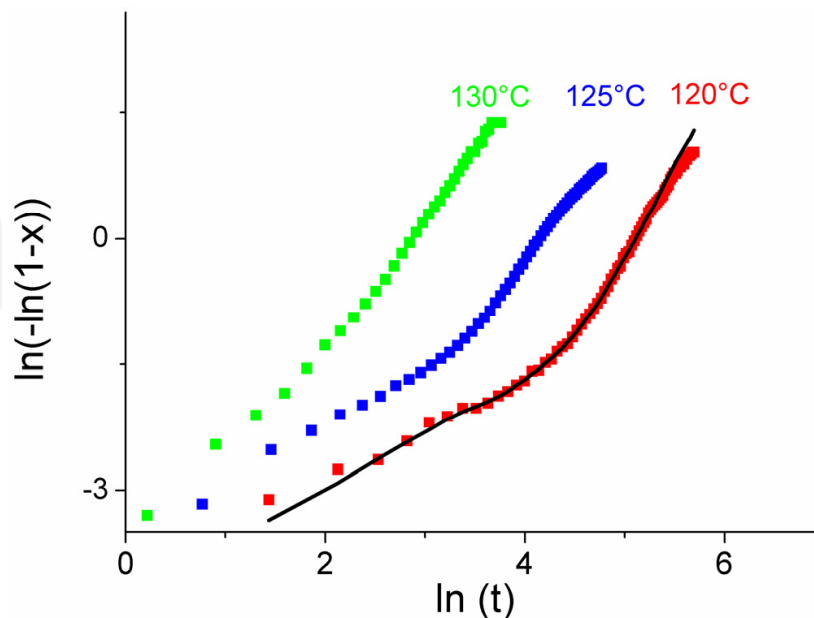


Fig. 15. Avrami plot of $\ln[-\ln(1-x)]$ vs $\ln(t)$ for $\text{Ge}_1\text{Sb}_2\text{Te}_4$ films. Points – experiment, black curve – results from fitting using equation (7).

Continuous black curves on Fig. 14 show the calculated the volume fractions of metastable $\text{Ge}_1\text{Sb}_4\text{Te}_7$ and stable $\text{Ge}_1\text{Sb}_2\text{Te}_4$ phase obtained from fittings using Equation (7). Results of simulation have shown that the same as in $\text{Ge}_2\text{Sb}_2\text{Te}_5$, the volume fraction of metastable $\text{Ge}_1\text{Sb}_4\text{Te}_7$ phase grows up to a maximum value and then decreases and disappears. After some incubation time, $\text{Ge}_1\text{Sb}_2\text{Te}_4$ phase began to growth and all material was transformed into a stable crystalline phase.

Additionally, the model is capable to simulate the JMAK plot of Fig. 15, in which the first slope of the JMAK plot can be related to the kinetic behavior of the metastable $\text{Ge}_1\text{Sb}_4\text{Te}_7$ phase.

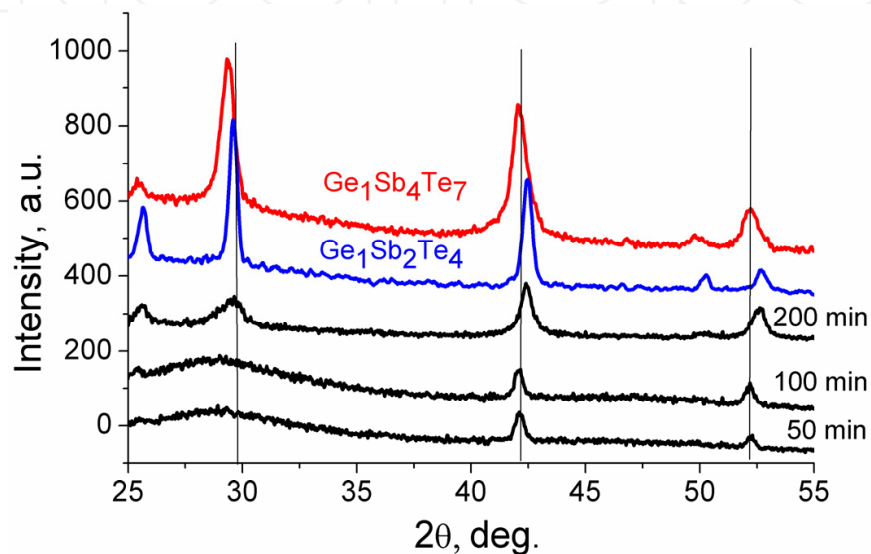


Fig. 16. X-ray diffraction spectra for a $\text{Ge}_1\text{Sb}_2\text{Te}_4$ film obtained in the process of isothermal annealing at a temperature of 120°C during the time indicated on the plot. Upper patterns correspond to $\text{Ge}_1\text{Sb}_4\text{Te}_7$ (red curve) and $\text{Ge}_1\text{Sb}_2\text{Te}_4$ (blue curve) taken at 180°C. The position of the $\text{Ge}_1\text{Sb}_4\text{Te}_7$ peaks is indicated with the vertical lines.

7. Crystallization of $\text{Ge}_1\text{Sb}_4\text{Te}_7$

Similarly, as with $\text{Ge}_2\text{Sb}_2\text{Te}_5$ and $\text{Ge}_1\text{Sb}_2\text{Te}_4$, $\text{Ge}_1\text{Sb}_4\text{Te}_7$ demonstrates a two phase transition: amorphous to the rock salt-like structure at a temperature of approximately 110°C and a second transition to the hexagonal phase at the temperature close to 168°C. This material demonstrates the fastest phase transformation among Ge:Sb:Te ternary alloys and phase-reversible transformations can be observed in the femtoseconds range (Huang et al., 2006). But because of the low crystallization temperature, $\text{Ge}_1\text{Sb}_4\text{Te}_7$ has lower thermal stability when compared with other ternary alloys (Miao et al., 2006).

Crystallization transformation from amorphous to NaCl-type structure in $\text{Ge}_1\text{Sb}_4\text{Te}_7$ differs from the transformations observed in $\text{Ge}_2\text{Sb}_2\text{Te}_5$ and $\text{Ge}_1\text{Sb}_2\text{Te}_4$ films. In contrast with $\text{Ge}_2\text{Sb}_2\text{Te}_5$ and $\text{Ge}_1\text{Sb}_2\text{Te}_4$, in-situ X-ray diffraction measurements show that amorphous films with the $\text{Ge}_1\text{Sb}_4\text{Te}_7$ composition crystallize in the NaCl-type phase with the same composition as at the beginning of the transformation (Figure 17). Moreover, isothermal reflection measurements (Figure 18) have shown practically zero value of crystalline phase during the much shorter incubation time compared with $\text{Ge}_2\text{Sb}_2\text{Te}_5$ films (Figure 11). In this

case, as is for GeTe and $\text{Ge}_4\text{Sb}_1\text{Te}_5$, it is also possible to neglect the amount of crystallized material during τ , and describe the transformation using the modified JMAK equation (3).

Figure 19 shows a plot of $\ln[-\ln(1-x)]$ versus $\ln(t-\tau)$ for a $\text{Ge}_1\text{Sb}_4\text{Te}_7$ film, which demonstrates a linear dependence. This means that the crystallization process in $\text{Ge}_1\text{Sb}_4\text{Te}_7$ material displays random nucleation and isotropic growth with effective activation energy of 1.7 ± 0.27 eV and an Avrami exponent n close to 1.94. According to (Christian, 1975), the values of n in the range $1.5 < n < 2.5$ correspond to a crystallization process dominated by all shapes growing from small dimensions with decreasing nucleation rate.

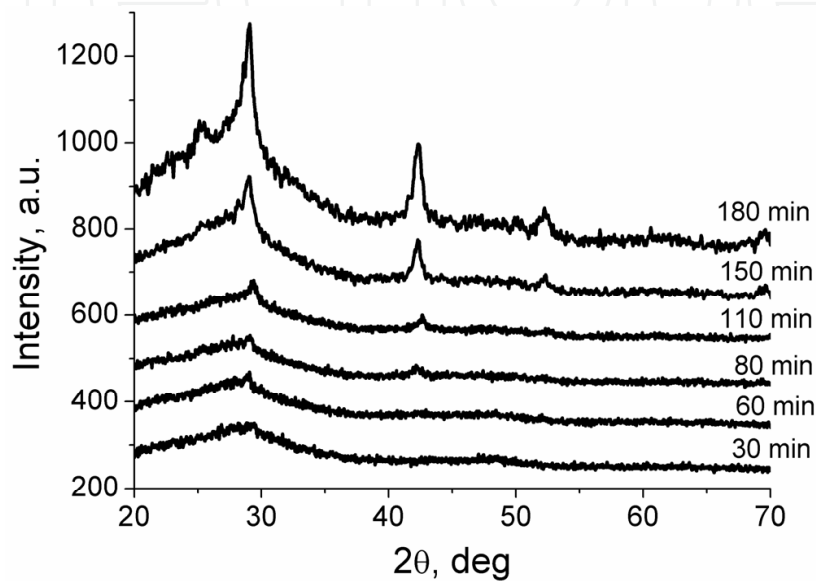


Fig. 17. X-ray diffraction spectra for a $\text{Ge}_1\text{Sb}_4\text{Te}_7$ film obtained in the process of isothermal annealing at a temperature of 90°C during the time indicated on the plot.

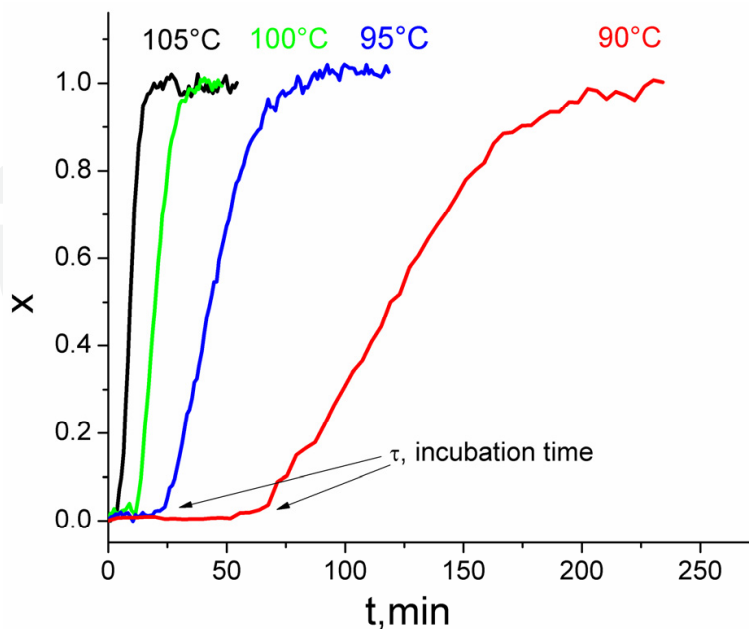


Fig. 18. Dependencies of the volume fraction x versus time obtained for $\text{Ge}_1\text{Sb}_4\text{Te}_7$ samples from reflection measurements at the temperature indicated on the graph.

8. Crystallization of Sb_2Te_3

Sb_2Te_3 lies at the end of the $\text{GeTe-Sb}_2\text{Te}_3$ pseudobinary line and has the lowest crystallization temperature but the highest crystallization speed. This material is an attractive candidate for phase change random access memory due to its rapid crystallization speed, but the crystallization temperature of Sb_2Te_3 (about 94°C in material investigated in this chapter and between $90\text{-}100^\circ\text{C}$ reported in the literature (Yin et al., 2007, Kim et al., 2010)) is too low for it to be of practical use.

Upon annealing, amorphous Sb_2Te_3 films crystallize in rhombohedral Sb_2Te_3 (Kim et al., 2008, Lv et al., 2010) or fcc structure, which at a temperature above 200°C transforms into an hexagonal phase (Yin et al., 2007, Zhu et al., 2011). In the investigated Sb_2Te_3 films within the temperature range comprised between $95\text{-}200^\circ\text{C}$, only the rhombohedral phase (JCPDS data #15-0874) has been observed.

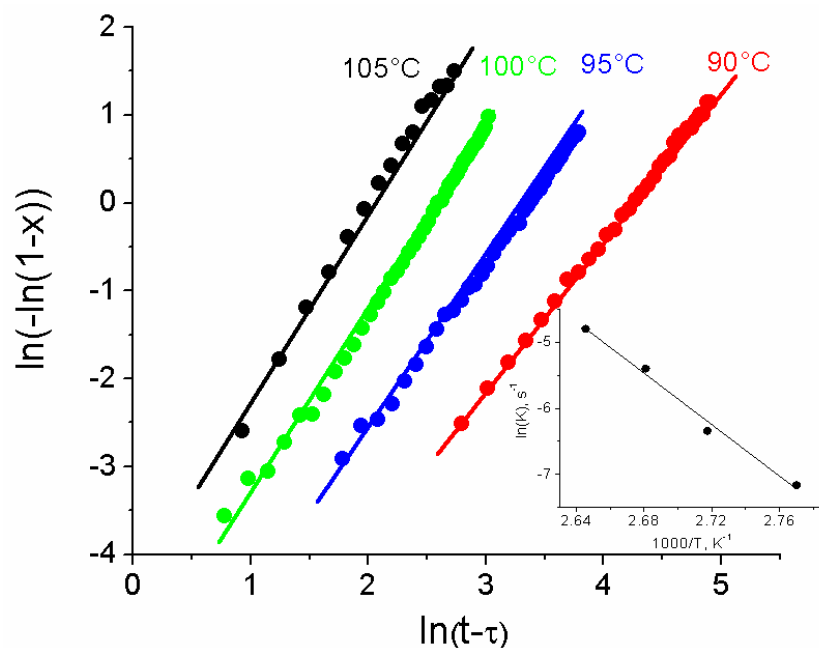


Fig. 19. Avrami plot of $\ln[-\ln(1-x)]$ vs $\ln(t-\tau)$ for $\text{Ge}_1\text{Sb}_4\text{Te}_7$ films. Points – experiment, lines – results from fittings using JMAK equation (3). Insert shows the rate constant K as a function of the reciprocal temperature.

Isothermal reflection measurements (Figure 20) have shown the same as for $\text{Ge}_1\text{Sb}_4\text{Te}_7$: practically zero value of crystalline phase during the incubation time. In this case, the same as for GeTe , $\text{Ge}_4\text{Sb}_1\text{Te}_5$ and $\text{Ge}_1\text{Sb}_4\text{Te}_7$ it is possible to neglect the amount of crystallized material during τ , and describe the transformation using the modified JMAK equation (3).

Figure 21 shows a plot of $\ln[-\ln(1-x)]$ versus $\ln(t-\tau)$ for a Sb_2Te_3 film, which demonstrates a linear dependence. This means that the crystallization process in Sb_2Te_3 films, the same as in $\text{Ge}_1\text{Sb}_4\text{Te}_7$ material, display random nucleation and isotropic growth with an effective activation energy of 1.54 ± 0.15 eV and an Avrami exponent n close to 1.1, which according to ref. (Christian, 1975), corresponds to a crystallization growth of particles of appreciable initial volume. It is necessary to note that the values obtained for crystallization activation energy is in good agreement with values reported in the literature (1.51 eV) obtained using

the Kissinger analysis in the films deposited on the glass substrates by the same DC magnetron sputtering (Zhai et al., 2009).

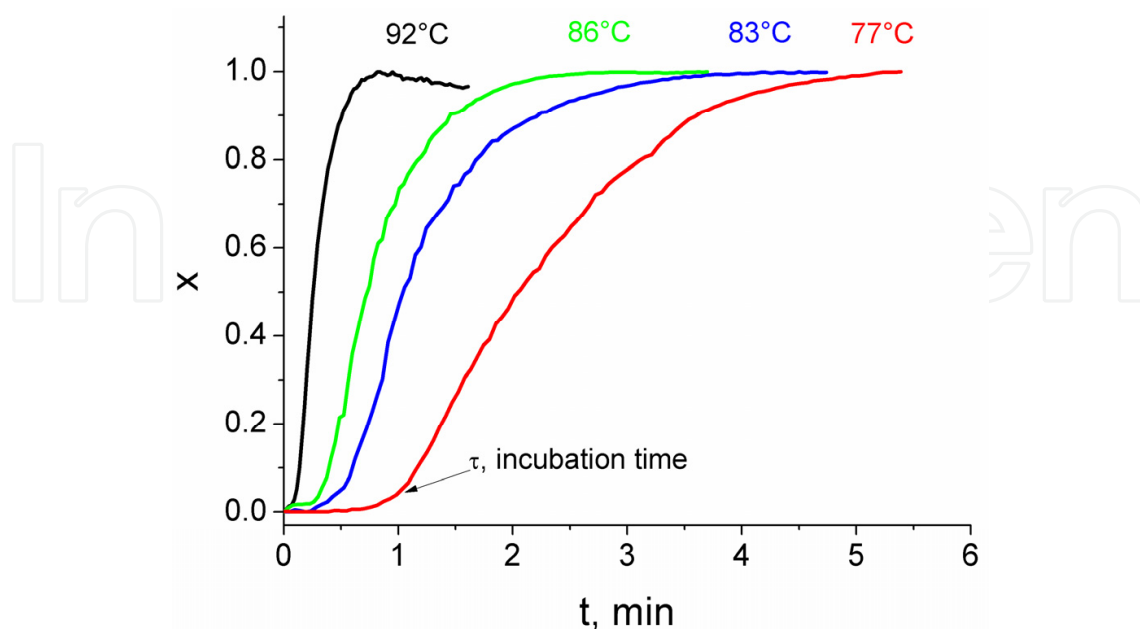


Fig. 20. Dependencies of the volume fraction x versus time obtained for Sb_2Te_3 samples from reflection measurements at the temperatures indicated on the graph.

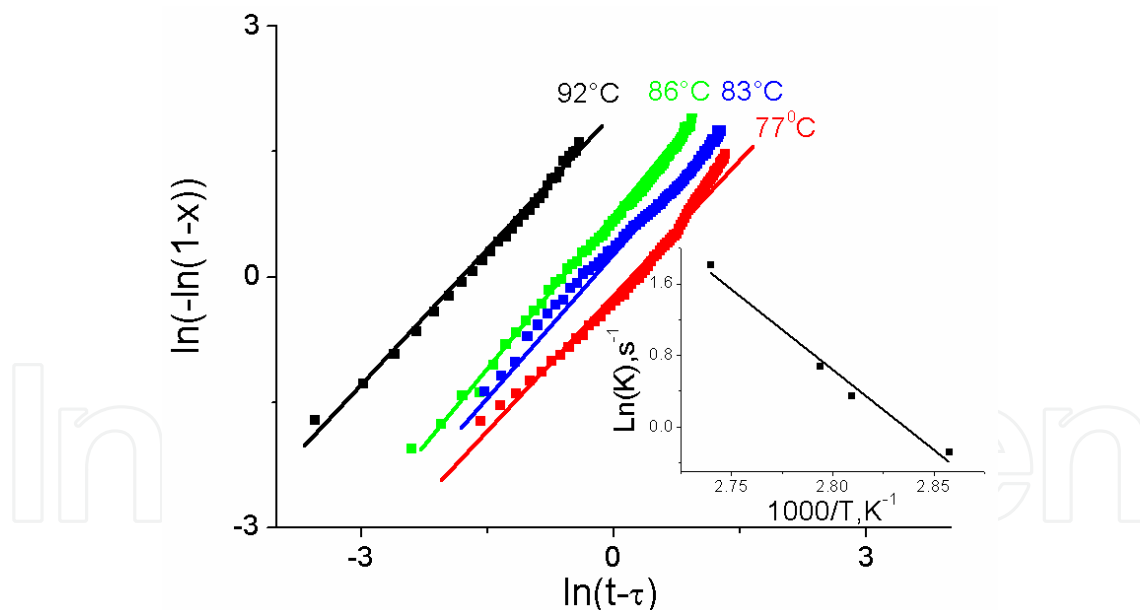


Fig. 21. Avrami plot of $\ln[-\ln(1-x)]$ vs $\ln(t-\tau)$ for Sb_2Te_3 films. Points - experiment, lines - results from fittings using JMAK equation (3). Insert shows the rate constant K as function of the reciprocal temperature.

9. Conclusions

This chapter presents some of the results concerning the crystallization properties of the most commonly employed materials on the GeTe- Sb_2Te_3 pseudo-binary line for phase

change memory application. Despite the fact that these alloys have found application in already commercialized optical disc and workable electrical phase change memory devices, their properties are not well known so far. This leads to many contradictory and controversial results in the literature.

As has been shown in this chapter, the crystallization properties of GeTe, Ge₄Sb₁Te₅, Ge₁Sb₄Te₇, and Sb₂Te₃ cannot be analyzed using the classical Johnson-Mehl-Avrami-Kolmogorov model for isothermal annealing due to the long incubation times. This limitation can be avoided by using a modification of the JMAK model, which takes into account that after incubation time the rate constant of crystallization can be considered as independent from time. Such model gave reasonable values of crystallization energy, which proved compatible with crystallization energy obtained by other methods. The difference in interpretation of isothermal measurements, in addition to the difference in preparation methods, can be responsible for the dispersion of crystallization parameters reported in the literature. But this modified model can be applied if during incubation time non-negligible amounts of crystalline phase material are observed. In the case of Ge₂Sb₂Te₅ and Ge₁Sb₂Te₄ films during incubation times, the nuclei fraction is of about 10% and has a composition corresponding to Ge₁Sb₄Te₇, which is different from the nominal value for the amorphous matrix. That is why the crystallization in Ge₂Sb₂Te₅ and Ge₁Sb₂Te₄ materials during isothermal annealing can be considered as a process that takes place in two stages: in the first stage, nuclei of a metastable Ge₁Sb₄Te₇ phase appear; in the second stage, the nuclei transforms into the equilibrium NaCl-type stoichiometric structures correspondent to the material composition. Such crystallization process can be described by a model in which the stable crystalline phase is preceded by the formation of a metastable phase. The most questionable issue is to explain these crystallization properties.

It is necessary to note that crystallization with phase separation has been observed in materials close to the GeTe-Sb₂Te₃ pseudo-binary line with excess of Ge (Ge_{2+x}Sb₂Te₅ x=0.5 (Privitera et al., 2003) and Sb (Ge₂Sb_{2+x}Te₅, 0<x<1, (Yamada et al., 2000), and Ge₂Sb_{2.3}Te₅ (Yao et al., 2003)). In all of these materials, separation occurs during the crystallization phase, with segregation of small amounts of the excess elements, which remain in the amorphous state at the grain boundaries. By increasing the annealing temperature, the residual amorphous material can convert into another polycrystalline NaCl-type structure with a slightly lower lattice parameter. As a result, after the formation of the first phase, the crystallization rate is strongly reduced and a further conversion of the film into another crystalline structure that crystallizes at higher temperatures can occur (Privitera et al., 2003).

Furthermore, Ge₂Sb₂Te₅, Ge₁Sb₂Te₄ and Ge₁Sb₄Te₇ materials crystallize into the same NaCl-type (*Fm* $\bar{3}$ *m*) structure (Matsunaga et al., 2004, Matsunaga et al., 2006) with lattice constants of 6.001, 6.044 and 6.0876 Å respectively (Morales-Sanchez et al., 2005). In materials with excess Sb, as the content of Sb increases, the lattice constant also increases (Yamada et al., 2000). Thus, during crystallization, atoms in the amorphous state must travel less distance to take their position in the Ge₁Sb₄Te₇ crystal lattice than in any other ternary alloys. This effect is responsible for the highest crystallization speed of Ge₁Sb₄Te₇ when compared with Ge₂Sb₂Te₅ and Ge₁Sb₂Te₄ materials. Also, Ge₁Sb₄Te₇ has the lowest crystallization

temperature. All these factors and the possible existence of a local composition fluctuation can be responsible for the appearance of $\text{Ge}_1\text{Sb}_4\text{Te}_7$ nuclei in the process of crystallization in $\text{Ge}_2\text{Sb}_2\text{Te}_5$ and $\text{Ge}_1\text{Sb}_2\text{Te}_4$ materials.

The clarification of crystallization mechanisms in alloys that lie on the $\text{GeTe-Sb}_2\text{Te}_3$ pseudo-binary line will allow the production of phase-change materials with better recording properties.

10. References

- Bahgat, A. A., Mahmoud, E. A., Abd, Rabo, A. S. & Mahdy, I. A. (2006). Study of the ferroelectric properties of Ge-Sb-Te alloys. *Physica B: Condensed Matter*, 382 No. 1-2, (April 2006) 271-278, ISSN 0921-4526.
- Caravati, S., Bernasconi, M. & Parrinello, M. First principles study of the optical contrast in phase change materials. *Journal of Physics: Condensed Matter*, 22, No. 31, (July 2010) 315801, ISSN 0953-8984.
- Claudio, D., Gonzalez-Hernandez, J., Licea, O., Laine, B., Prokhorov, E. & Trapaga, G. (2006) An analytical model to represent crystallization kinetics in materials with metastable phase formation. *Journal of Non-Crystalline Solids*, 352, No. 1, (January 2006) 51-55, ISSN 0022-3093.
- Christian, J. W. *The Theory of Transformation in Metals and Alloys*, (1975), Pergamon Press, Oxford. ISBN 978-0-08-044019-4, United Kingdom.
- Coombs, J. H., Jongenelis, A. P. J. M., Van Es-Spiekman, W. & Jacobs, B. A. (1995). Laser induced crystallization phenomena in GeTe based alloys. II. Composition dependence of nucleation and growth. *Journal of Applied Physics*, 78, No. 8, (October 1995) 4918-4956, ISSN 0021-8979.
- Fan, Z., Wang, L. & Laughlin, D. E. (2004). Modeling of Crystallization Activation Energy for GeTe-Sb₂Te₃ Based Phase Change Materials. *Proceedings of SPIE*, ISBN 0-8194-5293-9, Monterey CA. USA, April 2004.
- Fantini, A., Sousa, V. Perniola, L., Gourvest, E., Bastien, J. C., Maitrejean, S., Braga, S., Pashkov, N., Bastard, A., Hyot, B., Roule, A., Persico, A., Feldis, H., Jahan, C., Nodin, J. F., Blachier, D., Toffoli, A., Reibold, G., Fillot, F., Pierre, F., Annunziata, R., Benshael, D., Mazoyer, P., Vallee, C., Billon, T., Hazart, J., De Salvo, B. & Boulanger, F. (2010). N-doped GeTe as Performance Booster for Embedded Phase-Change Memories. *Proceedings of International Electron Device Meeting (IEDM)*. ISBN 978-1-4424-7418-5, San Francisco, CA. USA, December 2010.
- Gervacio, Arciniega, J. J., Prokhorov, E., Espinoza, Beltran, F. J. & Gonzalez-Hernandez, J. (2010). Ferroelectric properties of $\text{Ge}_2\text{Sb}_2\text{Te}_5$ phase-change films. *Applied Physics Letters*, 97, No. 6, (August 2010) 063504, ISSN 0003-6951.
- Gonzalez-Hernandez, J., Chao, B. S., Strand, D., Ovshinsky, S. R., Pawlik, D. & Gasiorowski, P. (1992). Crystallization studies of GeSbTe optical memory materials. *Applied Physics Communications*, 11, No. 4, (April 1992) 557-581, ISSN 0277-9374.
- Henderson, D.W. (1979). Thermal analysis of non-isothermal crystallization kinetics in glass forming liquids. *Journal of Non-Crystalline Solids*, 30, No. 3, (July 1979) 301-315, ISSN 0022-3093.

- Huang, S. M., Huang, S. Y., Zhao, Z. J. & Sun, Z. (2006). Investigation of phase changes in $\text{Ge}_1\text{Sb}_4\text{Te}_7$ films by single ultra-fast laser pulses. *Applied Physics A*, 82, No. 3, (March 2006) 529–533, ISSN 0947-8396.
- Im, J., Eom, J. H., Park, C., Park, K., Suh, D. S., Kim, K., Kang, Y. S., Kim, C., Lee, T. Y., Khang, Y., Yoon, Y. G. & Ihm, J. (2008). Hierarchical structure and phase transition of $(\text{GeTe})_n(\text{Sb}_2\text{Te}_3)_m$ used for phase-change memory. *Physical Review B*, 78, No. 20, (November 2008) 205205, ISSN 1098-0121.
- Kalb, J., Spaepen, F. & Wuttig, M. (2004). Atomic force microscopy measurements of crystal nucleation and growth rates in thin films of amorphous Te alloys. *Applied Physics Letters*, 84, No. 25, (June 2004), 5240–5242, ISSN 0003-6951.
- Kato, N., Takeda, Y., Fukano, T., Motohiro, T., Kawai, S. & Kuno, H. (1999). Compositional Dependence of Optical Constants and Microstructures of GeSbTe Thin Films for Compact-Disc-Rewritable (CD-RW) Readable with Conventional CD-ROM Drives *Japanese Journal of Applied Physics*, 38, No. 3B, (March 1999) 1707-1708, ISSN 0021-4922.
- Khulbe P. K., Wright, E. M. & Mansuripur, M. (2000). Crystallization behavior of as-deposited, melt quenched, and primed amorphous states of $\text{Ge}_2\text{Sb}_{2.3}\text{Te}_5$ films. *Journal of Applied Physics*, 88, No. 7, (October 2000) 3926-3933, ISSN 0021-8979.
- Kim M. S., Cho, S. H., Hong, S. K., Roh, J. S. & Choi, D. J. (2008). Crystallization characteristics of nitrogen-doped Sb_2Te_3 films for PRAM application. *Ceramics International*, 34, No. 4, (May 2008) 1043–1046. ISSN 0272-8842.
- Kim, M.Y. & Oh, T. S. (2010). Crystallization behavior and thermoelectric characteristics of the electrodeposited Sb_2Te_3 thin films. *Thin Solid Films*, 518, No. 22, (September 2010) 6550-6553, ISSN 0040-6090.
- Kolobov, A. V., Fons, P., Frenkel, A. I., Ankudinov, A. L., Tominaga, J. & Uruga, T. (2004). Understanding the phase-change mechanism of rewritable optical media. *Nature Materials*, 3, (September 2004) 703-708, ISSN 1476-1122.
- Kolobov, A. V., Fons, P., Tominaga, J., Ankudinov, A. L., Yannopoulos, S. N. & Andrikopoulos, K. S. (2004). Crystallization-induced short-range order changes in amorphous GeTe. *Journal of Physics: Condensed Matter*, 16, No. 44, (October 2004) S5103–S5108, ISSN 0953-8984.
- Kolobov, A. V., Fons, P., Tominaga, J. & Uruga, T. (2006). Why DVDs work the way they do: The nanometer-scale mechanism of phase change in Ge-Sb-Te alloys. *Journal of Non-Crystalline Solids*, 352, No. 9-20, (March 2006) 1612–1615, ISSN 0022-3093.
- Kyrsta, S., Cremer, R., Neuschütz, D., Laurenzis, M., Bolivar, P. H. & Kurz, H. (2001). Deposition and characterization of Ge-Sb-Te layers for applications in optical data storage. *Applied Surface Science*, 179, No.1-4, (July 2001) 55-60, ISSN 0169-4332.
- Laine, B., Trapaga, G., Prokhorov, E., Morales-Sanchez, E. & Gonzalez-Hernandez, J. (2003). Model for isothermal crystallization kinetics with metastable phase formation. *Applied Physics Letters*, 83, No. 24, (December 2003) 4969–4971, ISSN 0003-6951.
- Libera M. & Chen, M. (1993). Time-resolved reflection and transmission studies of amorphous Ge-Te thin-film crystallization. *Journal of Applied Physics*, 73, No. 5, (March 1993) 2272-2282, ISSN 0021-8979.

- Liu, D., Xu, L., Liao, Y. B., Dai, M., Zhao, L., ...Xu, J., Wu, L. C., Ma, Z. Y. & Chen, K. J. (2006). Comparison of Thermal Stability and Electrical Characterization between $\text{Ge}_2\text{Sb}_2\text{Te}_5$ and $\text{Ge}_1\text{Sb}_2\text{Te}_4$ Phase-Change Materials. *Japanese Journal of Applied Physics*, 48, No. 12, (December 2009) 121104, ISSN 0021-4922.
- Lu Q. M. & Libera, M. (1995). Microstructural measurements of amorphous GeTe crystallization by hot-stage optical microscopy. *Journal of Applied Physics*, 77, No. 2, (January 1995) 517-521, ISSN 0021-8979.
- Lv, B., Hu, S., Li, W., Di, X., Feng, L., Zhang, J., Wu, L., Cai, Y., Li, B. & Lei, Z. (2010). Preparation and Characterization of Sb_2Te_3 Thin Films by Coevaporation. *International Journal of Photoenergy*, Article ID 476589 (June 2010), ISSN 1110-662X.
- Matsunaga, T., Kojima, R., Yamada, N., Kifune, K., Kubota, Y., Tabata, Y. & Takata, M. (2006). Single Structure Widely Distributed in a GeTe- Sb_2Te_3 Pseudobinary System: A Rock Salt Structure is Retained by Intrinsically Containing an Enormous Number of Vacancies within Its crystal, *Inorganic Chemistry*, 45, No. 5, (February 2006) 2235-2241, ISSN 0020-1669.
- Matsunaga, T. & Yamada, N. (2004). Structural investigation of GeSb_2Te_4 : A high-speed phase-change material. *Physical Review B*, 69, No. 10, (March 2004) 104111, ISSN 1098-0121.
- Matsushita, T., Nakau, T., Suzuki, A. & Okuda, M. (1989). Measurements of activation energy in the initialization process of amorphous GeTe films. *Journal of Non-Crystalline Solids*, 112, No. 1-3, (October 1989) 211-214, ISSN 0022-3093.
- Miao, X. S., Shi, L. P., Lee, H. K., Li, J. M., Zhao, R., Tan, P. K., Lim, K. G., Yang, H. X. & Chong, T. C. (2006). Temperature Dependence of Phase-Change Random Access Memory Cell. *Japanese Journal of Applied Physics*, 45, No. 5A, (May 2006), 3955-3958, ISSN 0021-4922.
- Morales-Sanchez, E., Lain, B., Prokhorov, E., Hernandez-Landaverde, M. A., Trapaga, G. & Gonzalez-Hernandez, J. (2010). Crystallization process in $\text{Ge}_2\text{Sb}_2\text{Te}_5$ amorphous Films. *Vacuum*, 84, No. 7, (March 2010) 877-881, ISSN 0042-207X.
- Morales-Sanchez, E., Prokhorov, E., Gonzalez-Hernandez, J. & Mendoza-Galvan, A. (2005). Structural, electric and kinetic parameters of ternary alloys of GeSbTe. *Thin Solid Films*, 471, No. 1-2, (January 2005) 243-247, ISSN 0040-6090.
- Naito, M., Ishimaru, M. & Hirotsu, Y. (2004). Local structure analysis of Ge-Sb-Te phase change materials using high-resolution electron microscopy and nanobeam diffraction. *Journal of Applied Physics*, 95, No. 12, (June 2004) 8130-8135, ISSN 0021-8979.
- Nobukuni N., Takashima, M., Ohno, T. & Horiea, M. (1995). Microstructural changes in GeSbTe film during repetitious overwriting in phase change optical recording. *Journal of Applied Physics*, 78, No. 12, (December 1995) 6980-6988, ISSN 0021-8979.
- Ohta, T., Inoue, K., Uchida, M., Yoshida, K., Akiyama, T., Furakawa, S., Nagata, K. & Nakamura, S. Phase change disk media having rapid cooling structure. *Japanese Journal of Applied Physics*, 28, Suppl. 28, No. 3, (March 1989) 123-128, ISSN 0021-4922.

- Okura, M., Naito, H. & Matsushita, T. (1992). Discussion on the Mechanism of Reversible Phase Change Optical Recording. *Japanese Journal of Applied Physics*, 31, No. 2B, (February 1992) 466-470, ISSN 0021-4922.
- Ovshinsky S. R. (1968). Reversible electrical switching phenomena in disordered structures, *Physical Review Letters*, 21, No. 20, (November 1968) 1450-1453, ISSN 0031-9007.
- Ovshinsky, S. & P. Klose, Reversible High-Speed High-Resolution Imaging in Amorphous Semiconductors, *Society for Information Display International Symposium Digest of Technical Papers*, First Edition, 58-61 (1971).
- Paesler, M. A., Baker, D. A., Lucovsky, G., Edwards, A. E. & Taylor, P.C. (2007). EXAFS study of local order in the amorphous chalcogenide semiconductor $\text{Ge}_2\text{Sb}_2\text{Te}_5$. *Journal of Physics and Chemistry of Solids*, 68, No. 5-6, (March 2007) 873-877, ISSN 0022-3697.
- Park, J., Kim, M. R., Choi, W. S., Seo, H. & Yeon, C. (1999). Characterization of Amorphous Phases of $\text{Ge}_2\text{Sb}_2\text{Te}_5$ Phase-Change Optical Recording Material on Their Crystallization Behavior. *Japanese Journal of Applied Physics*, 38, No. 8, (May 1999) 4775-4779, ISSN 0021-4922.
- Perniola, L., Sousa, V., Fantini, A., Arbaoui, E., Bastard, A., Armand, M., Fargeix, A., Jahan, C., Nodin, J.-F., Persico, A., Blachier, D., Toffoli, A., Loubriat, S., Gourvest, E., Betti, Beneventi, G., Feldis, H., Maitrejean, S., Lhostis, S., Roule, A., Cueto, O., Reibold, G., Poupinet, L., Billon, T., De Salvo, B., Bensahel, D., Mazoyer, P., Annunziata, R., Zuliani, P. & Boulanger, F. (2010). Electrical Behavior of Phase-Change Memory Cells Based on GeTe. *Electron Device Letters IEEE*, 31, No. 5, (April 2010) 488-490, ISSN 0741-3106.
- Popescu, M. A. Ovonic Materials. (2005). *Journal of Ovonic Research*, 1, No. 6, (December 2005), 69-76, ISSN 1584-9953.
- Privitera, S., Rimini, E., Bongiorno, C., Zonca, R., Pirovano, A. & Bez, R. (2003). Crystallization and phase separation. in $\text{Ge}_{2+x}\text{Sb}_2\text{Te}_5$ thin Films. *Journal of Applied Physics*, 94, No. 7, (October 2003) 4409-4413, ISSN 0021-8979.
- Rabe, K. & Joannopoulos, J. (1987). Theory of the structural phase transition of GeTe. *Physical Review B*, 36, No. 12, (October 1987) 6631-6639, ISSN 1098-0121.
- Raoux, S., Shelby, R. M., Jordan-Sweet, J., Munoz, B., Salinga, M., Chen, Y. C., Shih, Y.H., Lai, E. K. & Lee, M.H. (2008). Phase change materials and their application to random access memory technology. *Microelectronic Engineering*, 85, No. 12, (August 2008) 2330-2333, ISSN 0167-9317.
- Reddy, G. B., Dhar, A., Malhotra L. K. & Sharmila E. K. (1992). Comparative study of crystallization processes in Sb₂Te₃ films using laser and thermal annealing techniques. *Thin Solid Films*, 220, No. 1-2, (1992) 111-115, ISSN 0040-6090.
- Ruitenbergh, G., Petford-Long, A. K. & Doole, R. C. (2002). Determination of the isothermal nucleation and growth parameters for the crystallization of thin $\text{Ge}_2\text{Sb}_2\text{Te}_5$ films. *Journal of Applied Physics*, 92, No. 6, (September 2002) 3166-3173, ISSN 0021-8979.
- Ruiz, Santos, R., Prokhorov, E., Espinoza, Beltran, F. J., Trapaga, Martinez, L. G. & Gonzalez-Hernandez, J. (2010). Crystallization and ferroelectric properties of $\text{Ge}_4\text{Sb}_1\text{Te}_5$ films. *Journal of Non-Crystalline Solids*, 356, No. 52-54, (July 2010) 3026-3031, ISSN 0022-3093.

- Senkader S. & Wright, C. D. (2004). Models for phase-change of $\text{Ge}_2\text{Sb}_2\text{Te}_5$ in optical and electrical memory devices. *Journal of Applied Physics*, 95, No. 2, (January 2004) 504-511, ISSN 0021-8979.
- Sian, T. S., Mittal, S., Goel, A., Chakraborty, S., Gautam, S., Budhwar, A., Kapil, R., Achar, P. C. & Nyati, G. (2008). Correlations between electrical parameters of rewritable digital versatile disc and optical and thermal properties of phase change alloy: effect of sputter power. *Japanese Journal of Applied Physics*, 47, No. 2, (February 2008) 936-941, ISSN 0021-4922.
- Strand, D. (2005). Ovonics: from science to products. *Journal of Optoelectronics and Advanced Materials*, 7, No. 4, (August 2005) 1679-1690, ISSN 1454-4164.
- Tominaga, J., Shima, T., Kuwahara, M., Fukaya, T., Kolobov, A. & Nakano, T. (2004). Ferroelectric catastrophe: beyond nanometre-scale optical resolution. *Nanotechnology*, 15, No. 5, (January 2004) 411-415, ISSN 0957-4484.
- Trappe, C., Bechvet, B., Hyot, B., Winkler, O., Facso, S. & Kurz, H. (2000). Recrystallization Dynamics of Phase Change Optical Disks with a Nitrogen Interface Layer. *Japanese Journal of Applied Physics*, 39, No. 2B, (February 2000) 766-769, ISSN 0021-4922.
- Wamwangi, D., Njoroge, W. K. & Wuttig, M. (2002). Crystallization kinetics of $\text{Ge}_4\text{Sb}_1\text{Te}_5$ films. *Thin Solid Films*, 408, No. 1-2, (March 2002) 310-315, ISSN 0040-6090.
- Weidenhof, V., Friedrich, I., Ziegler, S. & Wuttig, M. (2001). Laser induced crystallization of amorphous $\text{Ge}_2\text{Sb}_2\text{Te}_5$ films. *Journal of Applied Physics*, 89, No. 6, (March 2001) 3168-3176, ISSN 0021-8979.
- Wei J. & F. Gan. (2003). Theoretical explanation of different crystallization processes between as-deposited and melt-quenched amorphous $\text{Ge}_2\text{Sb}_2\text{Te}_5$ thin films. *Thin Solid Films*, 441, No. 1-2, (September 2003) 292-297, ISSN 0040-6090.
- Yamada, N. (1996). Erasable phase-change optical material, *MRS Bulletin*, 21, No. 9, (October 1996) 48-50, ISSN 0883-7694.
- Yamada, N. & Matsunaga, T. (2000) Structure of laser-crystallized $\text{Ge}_2\text{Sb}_{2+x}\text{Te}_5$ sputtered thin films for use in optical memory. *Journal of Applied Physics*, 88, No. 12, (December 2000) 7020-7028, ISSN 0021-8979.
- Yamada, N., Ohno, E., Nishiuchi, K., Akahira, N. & Takao, M. (1991). Rapid-phase transitions of GeTe-Sb, Te, pseudobinary amorphous thin films for an optical disk memory, *Journal of Applied Physics*, 69, No. 5, (March 1991) 2849-2856, ISSN 0021-8979.
- Yao, H. B., Shi, L. P., Chong, T. C., Tan, P. K. & Miao, X. S. (2003). Optical Transition of Chalcogenide Phase-Change Thin Films. *Japanese Journal of Applied Physics*, 42, No. 2B, (February 2003) 828-831, ISSN 0021-4922.
- Yin, Y., Sone H. & S. Hosaka. (2007). Characterization of nitrogen-doped Sb_2Te_3 films and their application to phase-change memory. *Journal of Applied Physics*, 102, No. 6, (September 2007) 064503, ISSN 0021-8979.
- Zhai, F., Wang, Y., Wu, Y. & Gan, F. (2009). Phase Transition Kinetics of Sb_2Te_3 Phase Change Thin Films. *Proceedings of SPIE*, ISBN 0-8194-5293-9 Wuhan, China, November 2008.
- Zhang, T., Cheng, Y., Song, Z., Liu, B., Feng, S., Han, X., Zhang, Z. & Chen, B. (2008). Comparison of the crystallization of Ge-Sb-Te and Si-Sb-Te in a constant-

temperature annealing process. *Scripta Materialia*, 58, No. 11, (February 2008) 977–980, ISSN 1359-6462.

Zhu, M., Wu, L., Rao, F., Song, Z., Peng, C., Li, X., Yao, D., Xi, W. & Feng, S. Phase Change Characteristics of SiO₂ Doped Sb₂Te₃ Materials for Phase Change Memory Application. *Electrochemical and Solid-State Letters*, 14, No. 10, (July 2011) H404-H407, ISSN 1099-0062.

IntechOpen

IntechOpen

© 2012 The Author(s). Licensee IntechOpen. This is an open access article distributed under the terms of the [Creative Commons Attribution 3.0 License](#), which permits unrestricted use, distribution, and reproduction in any medium, provided the original work is properly cited.

IntechOpen

IntechOpen